SemLayoutDiff: Semantic Layout Generation with Diffusion Model for Indoor Scene Synthesis

Xiaohao Sun 1 Divyam Goel 2 Angel X. Chang 1,3 1 Simon Fraser University 2 CMU 3 Alberta Machine Intelligence Institute (Amii)

3dlg-hcvc.github.io/SemLayoutDiff/



Figure 1. SEMLAYOUTDIFF generates 3D scenes conditioned on an architectural map or unconditionally. Left (full pipeline): With architectural conditioning and room type label, SEMLAYOUTDIFF synthesizes a 2D semantic layout map, predicts 3D attributes to form bounding box layouts, and retrieves objects to construct a final scene. Right: In the unconditional setting, SEMLAYOUTDIFF generates the architecture map and the semantic layout map from noise and room type label before synthesizing the scene (3D layout stage not shown).

Abstract

We present SemLayoutDiff, a unified model for synthesizing diverse 3D indoor scenes across multiple room types. The model introduces a scene layout representation combining a top-down semantic map and attributes for each object. Unlike prior approaches, which cannot condition on architectural constraints, SemLayoutDiff employs a categorical diffusion model capable of conditioning scene synthesis explicitly on room masks. It first generates a coherent semantic map, followed by a cross-attention-based network to predict furniture placements that respect the synthesized layout. Our method also accounts for architectural elements such as doors and windows, ensuring that generated furniture arrangements remain practical and unobstructed. Experiments on the 3D-FRONT dataset show that SemLayoutDiff produces spatially coherent, realistic, and varied scenes, outperforming previous methods.

1. Introduction

Automatic 3D indoor environment generation has many applications such as assisting content designers for AR/VR, video games, and serving as training data for computer vision models [29] and embodied AI agents [6]. Various approaches have been proposed for generating 3D indoor scenes. Typically, these methods separate the task into two steps: 1) generating a coarse layout specifying the seman-

tic categories and positions of objects, and 2) retrieving and placing suitable objects based on the generated layout.

Early attempts used design guidelines [25] to determine the object arrangement. These approaches used hand-crafted rules, limiting generalization to diverse types of scenes. Fisher et al. [9] introduced data-driven object placement. Since then, various deep learning techniques have been used for layout generation, including autoregressive models [27, 41, 43], graph neural networks [42], and diffusion over graphs [39]. More recently, LLMs have been used for open-vocabulary scene generation [1].

While LLMs are useful for providing priors on what objects are present and semantic relations between objects, they struggle to precisely place objects. Thus, researchers still actively investigate what can be learned via training on 3D scenes [16, 39]. Recent works trained on 3D scenes share common limitations: 1) room architecture is not handled, 2) interpenetration of objects, 3) lack of unified model that can be conditioned with different inputs (separate models typically trained for each room type).

To address the first two issues, we propose the use of a 2D top-down semantic map to represent the layout. In this semantic map, each cell represents one object category. By including architectural elements such as floors, doors, and windows, the representation also accommodates *generation of the room* as well as *layout of objects* in the room. The representation naturally ensures that objects do not overlap

and floorplan constraints are properly maintained as shown in related work [34, 53]. Specifically, we use a categorical diffusion model to generate the top-down semantic map. From the semantic map, we extract the object instances and their attributes (e.g., semantic category, size, orientation).

We also tackle training a unified model across room types that can be conditioned on the architecture and room type. We demonstrate that we can train a unified model that handles different room types and generates more plausible and realistic layouts. In summary, our contributions are:

- A novel scene representation using semantic layout maps with instance attributes, which enables simultaneous object placement and better captures spatial relationships
- A categorical diffusion model for scene synthesis by generating semantic maps, enabling a unified approach that
 efficiently handles diverse layouts across room types, captures architectural constraints and furniture relationships,
 and reduces out-of-bound and object intersection issues.
- Our model incorporates architectural elements by generating the room together with the objects, and conditioning on the architecture.

2. Related work

Rule-based and statistical prior indoor scene synthesis.

Early work relied on placement constraints [47] and rules based on interior design principles [25] to place objects. Following these works, Fisher et al. [9] learned object arrangements from a 3D scene database by modeling the co-occurrence and spatial relationship of pairs of objects and constructing scenes hierarchically based on support.

Deep-learning based scene synthesis. Wang et al. [41], introduced auto-regressive scene generation and used CNNs for scene synthesis by representing scenes as 2D top-down images, with multiple channels encoding information such as floor layout, object semantic mask, etc. Followup work improved generation efficiency [30], and used transformers to decode the objects [26, 27, 37, 43]. Scenes were also modeled using graphs: a scene-hierarchy [12, 20], a relationship graph [23, 42, 51, 54], or a hybrid representation that combines scene-graphs with top-down image based representation [53]. Recent work [21, 36, 39] trains denoising diffusion model to generate the scene graph, with some work incorporating a floor plan as a conditioning signal [16, 24] and loss terms to avoid collisions [49].

We advocate the use of 2D top-down images as in Wang et al. [41]. Instead of autoregressively adding one object at a time, we use diffusion to layout all objects together. By working directly in image space, the model can ensure that the position of the objects is within the floor plan. Concurrent to our work, Su et al. [34] used diffusion-based models to generate a semantic layout conditioned on floor plan, but uses continuous instead of discrete categorical outputs.

LLM/VLM-based scene generation. As LLMs and VLMs

capture common-sense knowledge about object placements in rooms, researchers developed frameworks that leverage LLMs to generate more open-world scenes based on text [3, 17, 45, 50] and/or visual information [35]. While the use of LLMs/VLMs is a promising direction, we investigate whether we can train a unified model that generates reasonable semantic layouts using diffusion.

Combined layout and object generation. With advances in 3D shape generation, recent work has studied how to generate objects for a specified layout using NeRF in a compositional setting [5, 22, 28]. Our model can be used to specify the initial layout used by these compositional approaches. Some works generate both the layout and the objects [11, 40, 51, 52], typically with a graph-based representation for the layout and then a shape generator for each object. Some [51, 52] still learn priors on the placement of objects from 3D datasets such as 3D-FRONT [10], while others [11] use an LLM to convert text to semantic scenegraphs, which are then used to generate relative positions of objects. We demonstrate in Fig. 8 that layouts generated by our model can also be combined with generated objects.

Diffusion models for layout generation. Diffusion has also been applied to 2D layout synthesis [14, 31–33]. Chai et al. [4] explore graphic layout generation with a newly designed transformer-based denoiser. Inoue et al. [18] formulate a discrete diffusion model for layout generation, which can solve diverse tasks via a single model using complex layout constraints. Another work [15] shows that using a multinomial diffusion model over categorical data, it is possible to generate 2D semantic maps. We take inspiration from diffusion for 2D layouts, and use diffusion to generate a 2D top-down semantic map that captures the spatial relationship between all objects.

3. Semantic Layout Representation

In recent scene generation work, the scene is represented as a sequence of objects [27] with corresponding attributes (category, location, etc.) or a scene graph [39] where nodes indicate objects and edges indicate object relations. Both approaches face the problem of overlapping objects and do not necessarily respect the floor boundary.

To tackle this problem, we represent the scene as a semantic map with exact instance annotation, shown in Fig. 2. The semantic map, denoted as $\mathcal{S} \in \mathbb{R}^{H \times W}$, represents the semantic segmentation of a top-down projection of a room, encoding both location and object category. Each pixel corresponds to fixed physical dimensions. We use a scale of s=0.01 meters (i.e., a pixel is 0.01 meters). We denote the instance-level annotations as $\mathcal{I}=\{O_i\}$ where i=1,...,N, where N is the total number of objects within the room. Each instance O_i is defined by $O_i=\{c_i,s_i,p_i,r_i\}$, representing an object's category, size, position, and orientation. The category $c_i \in \{0,1\}^K$ is a categorical variable over

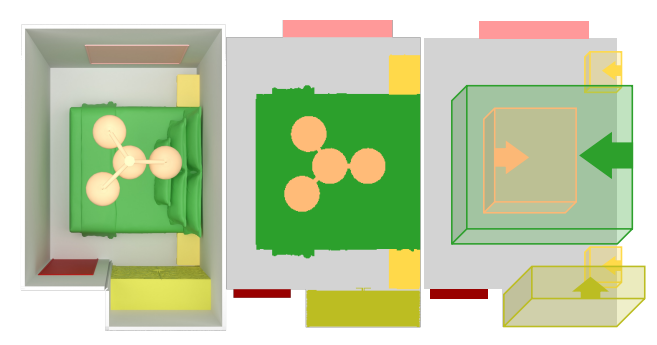


Figure 2. Semantic map representation example. We represent the scene in two parts: the 2D top-down semantic map with a fixed physical unit per pixel (middle) and the 3D bounding boxes with orientations for object-level attributes (right). Note that the left image is the corresponding rendered scene.

the total number of semantic categories K in the dataset, where K=C+4. Here, C is the number of object types, and the additional categories represent architectural elements: void (outside room boundaries), floor, door, and window. Including floors, doors, and windows enables our model to generate the room together with the objects, while also handling architectural constraints. Our framework can be simplified to scenarios without doors and windows by reducing the semantic categories to K=C+2, representing only floor and void. This simplified setting is similar to conditioning by floor as in prior work [16, 27]. However, our method simultaneously generates the room and object layouts, even under unconditional generation.

For each object instance O_i , in addition to the semantic category c_i , we also specify the bounding box size $s_i \in \mathbb{R}^3$, position $p_i \in \mathbb{R}^3$, and orientation r_i . For the orientation, we only consider the rotation of objects about the up (vertical) axis. From analyzing the orientation of objects in 3D-FRONT, we observed that over 97% of orientations are aligned with the coordinate axes. Thus we restrict our problem to predicting four distinct orientation classes and use a categorical variable $r_i \in \{0,1,2,3\}$ to indicate the object's front direction corresponding to $0^{\circ}, 90^{\circ}, 180^{\circ}, 270^{\circ}$.

We process the scene data using BlenderProc [7] to render top-down views of the rooms, producing both semantic map and instance-level annotations. The camera parameters ensure consistent pixel-to-meter scaling. Images are padded to a fixed size (1200×1200 , representing $12m \times 12m$). Finally, we apply the filtering strategy from ATISS [27] to ensure data quality. More details are in App. B.1.

4. Method

Unlike previous methods [16, 27, 39], our unified model generates all room types with a single model. It generates both the architecture and furniture objects at the same time in an unconditional way. Furthermore, it takes a *room mask* as input condition, and generates layouts conditioned on

just the floormask or the full architecture mask (archmask for short). Our model has two stages: 1) a semantic layout diffusion model (Fig. 3a) for predicting the layout, and 2) an attribute prediction model (Fig. 3b). The two stages are trained separately and combined at the inference stage.

4.1. Semantic Layout Generation

The first stage is based on the multinomial diffusion model [15], shown in Figure 3 (a). The multinomial diffusion model is a categorical discrete diffusion model designed for categorical data perfectly suited for our data representation. We modify the multinomial diffusion model to make it a unified model conditioned on possible room masks for all room types.

During training, the input is a 2D segmentation map $\mathcal{S} \in \mathbb{R}^{H \times W \times K}$, where pixels indicate semantic ID. Each pixel value is a one-hot vector $\mathbf{x} \in \{0,1\}^K$, where K is the number of categories. We set K=38 semantic categories with 34 for object types, 3 for architecture elements (floor, door, window), and 1 for void. For conditioning, we specify the room type c_{room} and the room mask $\mathcal{A} \in \mathbb{R}^{H \times W}$ where $\mathcal{A}_{i,j} \in \{0,1,2,3\}$ denotes void, floor, door, and window respectively. Note that we can also condition with the floor (i.e., the room mask without doors or windows), which can be expressed as a binary mask, or do unconditional generation of both the room architecture and the objects.

We denote the noise pixel value at time step t as $\mathbf{x}_t \in \{0,1\}^K$. If $\mathbf{x_t}$ belongs to category k, then $\mathbf{x}_{tk} = 1$ and $\mathbf{x}_{tj} = 0$ for $j \neq k$. The probability of $\mathbf{x_t}$ given $\mathbf{x_0}$ is

$$q(\mathbf{x_t}|\mathbf{x_0}) = \mathcal{C}(\mathbf{x_t}|\bar{\alpha}_t\mathbf{x_0} + (1 - \bar{\alpha}_t/K))$$

where \mathcal{C} is the categorical distribution with parameters $\alpha_t = 1 - \beta_t$ and $\bar{\alpha}_t = \prod_{\tau=1}^t \alpha_{\tau}$.

The objective of the multinomial diffusion model is to minimize the KL divergence of the categorical distribution between the generated data and ground truth, which is

$$L_{\text{MDM}} = \mathbb{E}_{\mathbf{x},t} \left[\text{KL} \left(q(\mathbf{x}_{t-1} | \mathbf{x}_{t}, \mathbf{x}_{0}), p(\mathbf{x}_{t-1} | \mathbf{x}_{t}, \mathcal{A}, c_{\text{room}}) \right) \right]$$

where $q(\mathbf{x}_{t-1}|\mathbf{x}_t, \mathbf{x}_0)$ is the ground-truth categorical posterior and $p(\mathbf{x}_{t-1}|\mathbf{x}_t, \mathcal{A}, c_{\text{room}})$ is the predicted distribution at time t-1 given previous time t distribution, room mask and room type condition. See Hoogeboom et al. [15] for details of the multinomial diffusion model.

Figure 3 shows how the room mask \mathcal{A} is passed through an embedding layer and an MLP to get the room mask embedding, then added to the $\mathbf{x_t}$ embedding to control denoising so the generated layout can respect the input mask. Furthermore, the room type c_{room} embedding is added to the timestep embedding to allow generating the desired room type. The embedding size for both the room mask and room type is 64. These two conditions allow a unified model for all room types that generates the room semantic layout with

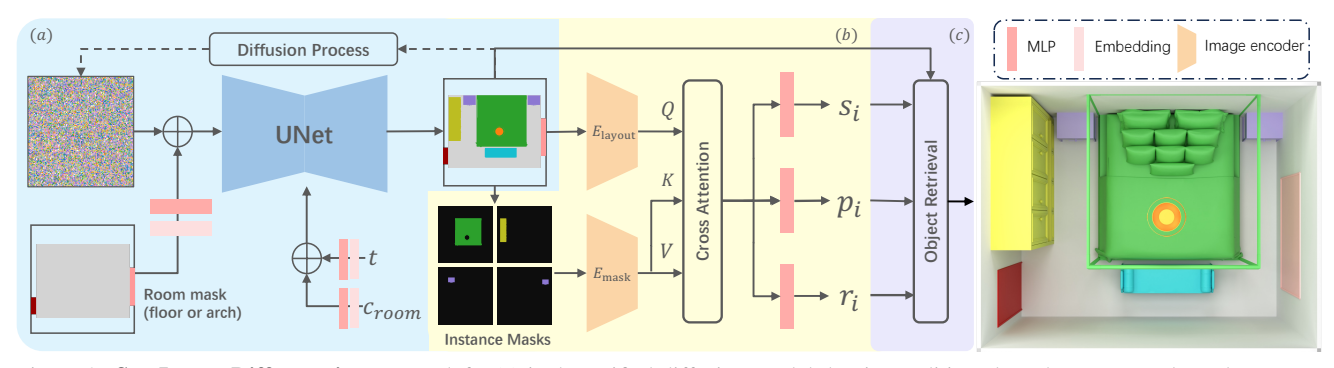


Figure 3. SemLayoutDiff overview. From left: (a) is the unified diffusion model that is conditioned on the room mask, and room type c_{room} . During the denoising process, the archmask or floormask embedding is added to the noise input embedding. The room type embedding is added to the timestep embedding. (b) is the object attribute prediction model with a semantic layout map as input. s_i, p_i, r_i indicate the ith instance's size, position, and orientation. At training time, we use ground-truth instance masks. During inference the semantic layout map is split into instance masks by using connected component analysis. The layout feature and the mask feature are passed to a cross-attention layer to get the final object instance feature, which is used to predict attributes. (c) During inference, objects are retrieved to match the category c_i and size s_i , and arranged using the position p_i and orientation r_i .

different room types and masks as input. By adding another control for the type of room mask used for conditioning (e.g., none, floor, arch), we can train a single unified model for all room and mask types (see App. D.4).

4.2. Attribute Prediction

The generated semantic layout only gives potential object instances and their 2D location on the projected plane. Thus, we design an attribute prediction model (APM) to predict attributes (s, p, r) for each object as shown in Figure 3 (b). Based on each instance mask, we obtain the 2D position and 2D size (width and length). The APM network then predicts the vertical size and position.

The input of the APM is the semantic map and the extracted instance masks, while the output is the instance-level object attributes, including vertical size $s_{y_i} \in \mathbb{R}^1$, vertical position $p_{y_i} \in \mathbb{R}^1$, and orientation $r_i \in \{0,1,2,3\}$. We pass the semantic layout map and instance mask to the encoder E_{layout} and E_{mask} respectively to get the layout feature $f_{\mathrm{layout}} \in \mathbb{R}^{128 \times 32 \times 32}$ and the instance mask feature $f_{\mathrm{mask}} \in \mathbb{R}^{128 \times 32 \times 32}$. We treat f_{layout} as the query and f_{mask} as the key and value to perform cross-attention to obtain the final object instance feature $f_{\text{inst}} \in \mathbb{R}^{128 \times 32 \times 32}$. Finally, we use different prediction heads, consisting of a shared 2layer MLP followed by a 1-layer MLP for each attribute, to predict attributes using f_{inst} . During training, we use the ground-truth instance masks. We use MSE loss for size and position heads, defined as L_s , L_p , and cross-entropy loss for orientation loss L_r . The total loss for the APM is a sum of the three losses: $L_{APM} = L_s + L_p + L_r$.

4.3. Inference

At inference, we follow the pipeline in Fig. 3 to generate the final scene (see App. A for details). Semantic layout sam**pling.** Given the room mask A and room type c_{room} as conditions, we sample a semantic layout map S using the semantic layout diffusion model. Instance extraction. Based on the generated semantic map S, we extract instances using connected component analysis. As there may be noisy pixels, we define category-specific size thresholds to filter out object instances that are too small. We determine the category-specific thresholds by calculating the minimum ratio of object pixels to total room pixels per object type. If an object's pixel ratio falls below the type-specific threshold, it is deemed invalid and excluded from subsequent attribute prediction and object retrieval. Attribute prediction. After we have both the semantic map and instance masks, we pass them to the attribute prediction model to predict attributes for each instance. Room construction and object **retrieval.** Lastly, we use the attributes to retrieve and place the objects. For unconditioned generation, we also construct the room based on the generated architecture mask.

5. Experiments

We compare our SEMLAYOUTDIFF with two recent diffusion methods (DIFFUSCENE, MIDIFFUSION). See App. B for additional experimental and training details.

Experimental protocol. We use the experimental setup from prior work [27, 39], but we revisit the evaluation protocol and show that rendering choices can greatly influence common evaluation metrics for scene generation (App. C). We advocate for a specific set of choices (rendering using a unified color palette that groups semantically close objects together, with a floormask, and shows more object details). **Dataset.** We train our model using the 3D-Front [10] training split from ATISS [27] with 4616 rooms containing bedrooms, living rooms, and dining rooms. We use 38 semantic classes (34 object types, 3 arch-element types, and void). **Baselines.** We select two recent diffusion-based indoor scene synthesis methods [16, 39] with training code for

comparison. We do not compare against CHoRD [34] as



Figure 4. Example textured synthesized scenes with unconditional generation. We generate the room architecture together with the placement of the objects.

there is no code available, and report results for a pretrained PhyScene [49] model in App. D.6. Note that MIDIFFUSION was originally designed to support floormask conditioning, while DIFFUSCENE do not. In addition, both works trained separate models for each room type. For fair comparison, we add room-type conditioning to prior methods (see App. B.3 for implementation details), and consider three generation modes for room mask conditioning: no room mask (none), conditioned on the floor, and architecture.

5.1. Examples of generated scenes

To demonstrate our model's ability to generate plausible room layouts, we show examples of generated rooms (objects and the room itself) in Fig. 4. We also compare generated scenes from our SEMLAYOUTDIFF to those generated by DIFFUSCENE and MIDIFFUSION with the three generation modes: no room mask (Fig. 5), conditioned on floor (appendix Fig. D.8), and on architecture (Fig. 6). For the comparison, we use semantically colored renderings with orthographic projection to clearly show the layout (see App. C). These are the same renderings used in the quantitative evaluation and user studies. We provide additional qualitative results and renderings in App. D.8.

SEMLAYOUTDIFF can generate the architecture mask without conditioning. In Fig. 5, we show examples of different rooms generated by our SEMLAYOUTDIFF and other methods. As prior methods (DIFFUSCENE, MIDIFFUSION) cannot generate the architecture mask, we show the scenes with a square floor. In contrast, our proposed SEMLAYOUTDIFF effectively generates diverse and realistic arch masks (including floors, doors, and windows) even without explicit architectural conditioning. The scenes produced by SEMLAYOUTDIFF exhibit more plausible and varied room shapes and furniture placements, highlighting its capability to create coherent indoor scenes.

SEMLAYOUTDIFF respects the architecture mask better. From Fig. 6, we observe that DIFFUSCENE and MID-IFFUSION struggle to place furniture with respect to archi-

Table 1. **Distribution match to ground-truth scenes.** We report the FID \downarrow , KID \downarrow , SCA%, and CKL \downarrow with different levels of architecture conditioning: unconditioned (None), conditioned on the floor (Floor), and the architecture map (Arch). **Bold** indicates best results. Our SEMLAYOUTDIFF outperforms other methods.

Condition	Method	FID↓	KID↓	SCA%	CKL↓
	DIFFUSCENE [39]	125.46	88.09	99.75	24.70
N	MIDIFFUSION [16]	100.54	41.27	97.35	28.31
None	SEMLAYOUTDIFF (Ours)	93.93	10.72	96.76	17.21
	DIFFUSCENE [39]	90.82	30.13	94.43	23.93
E1	MIDIFFUSION [16]	91.79	26.23	97.27	23.64
Floor	SEMLAYOUTDIFF (Ours)	81.79	14.52	89.83	5.99
	DIFFUSCENE [39]	88.47	30.22	95.02	20.42
Arch	MIDIFFUSION [16]	93.51	31.06	95.28	36.97
	SEMLAYOUTDIFF (Ours)	71.06	8.65	86.96	4.78

Table 2. **Physical plausibility of generated scenes.** We compare out-of-bounds (OOB) ratios at the scene (OOB_S \downarrow) and object level (OOB_O \downarrow), as well as the collision rate (COL \downarrow), and navigability (NAV \uparrow). We do not include DIFFUSCENE and MIDIFFUSION for the none condition as they do not generate any room architecture, so most of the metrics are irrelevant.

Condition	Method	$OOB_S \downarrow$	$OOB_O \downarrow$	COL↓	NAV↑
None	SEMLAYOUTDIFF (Ours)	2.04	0.46	17.70	95.30
	DIFFUSCENE [39]	69.93	28.92	37.68	94.99
Floor	MIDIFFUSION [16]	70.17	31.83	35.92	96.02
	SEMLAYOUTDIFF (Ours)	24.60	6.93	19.61	96.69
	DIFFUSCENE [39]	66.47	20.03	40.97	94.34
Arch	MIDIFFUSION [16]	60.68	34.66	51.62	96.19
	SEMLAYOUTDIFF (Ours)	16.63	6.62	16.13	96.36

tectural elements, often resulting in objects blocking doors, windows, or extending beyond room boundaries. In contrast, our proposed SEMLAYOUTDIFF consistently generates coherent, organized, and realistic furniture arrangements, effectively respecting architectural constraints such as doors, windows, and floor boundaries.

5.2. Quantitative evaluation

We evaluate the generated scenes by comparing against the distribution of real scenes, and evaluating the overall plausibility based on object collisions and how well the room mask is respected. For each condition, we generate 1000 scenes for evaluation.

Metrics. For comparison of synthesized and real scenes, we follow ATISS [27] and report the KL divergence (CKL) between object category distributions, and Fréchet inception distance (FID) [13] and Kernel inception distance (KID) [2] against the test set. Following prior work, we report the CKL as CKL $\times 10^2$ and the KID as KID $\times 10^3$. We also report the scene classification accuracy (SCA), which scores how well a trained classifier can distinguish synthesized scenes from real-world scenes.

For SCA, the closer the score is to 50%, the more difficult it is for the classifier to distinguish between generated and real scenes. We find that in our experiments, the se-

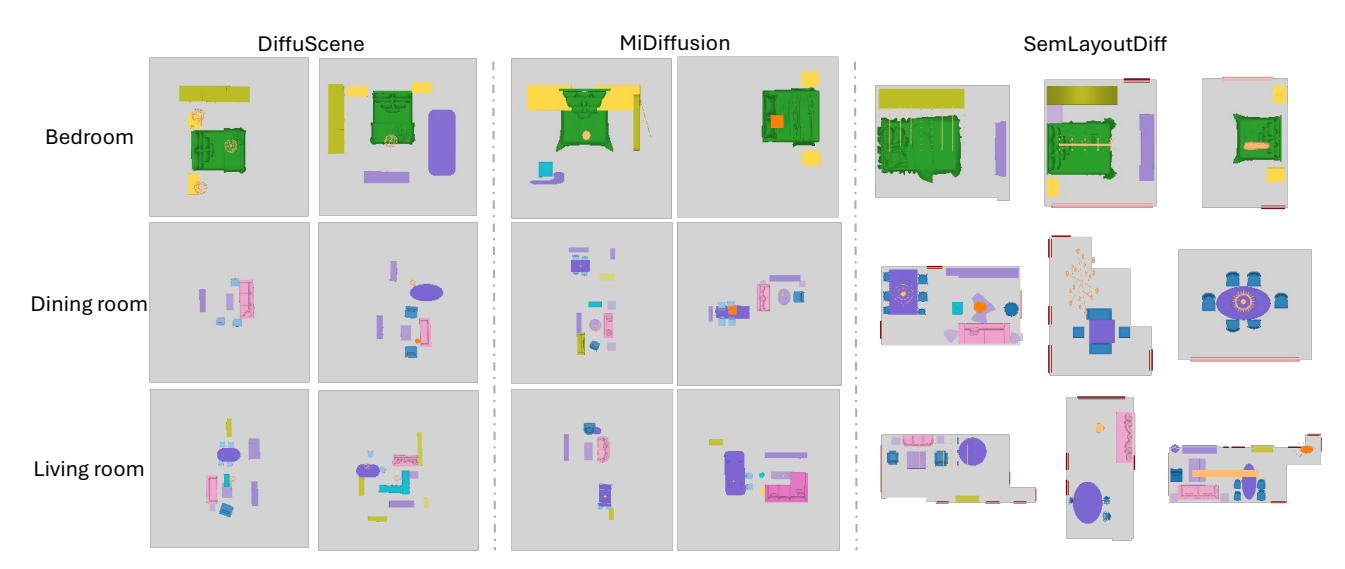


Figure 5. Comparison of scenes generated by prior methods and SEMLAYOUTDIFF without room mask (i.e., no floor or arch) conditioning. Since prior methods (left) cannot generate architectural elements, a square floor is used by default. Our method (right) generates feasible furniture placements aligned with its generated architectural layouts, leaving doors and windows unobstructed.

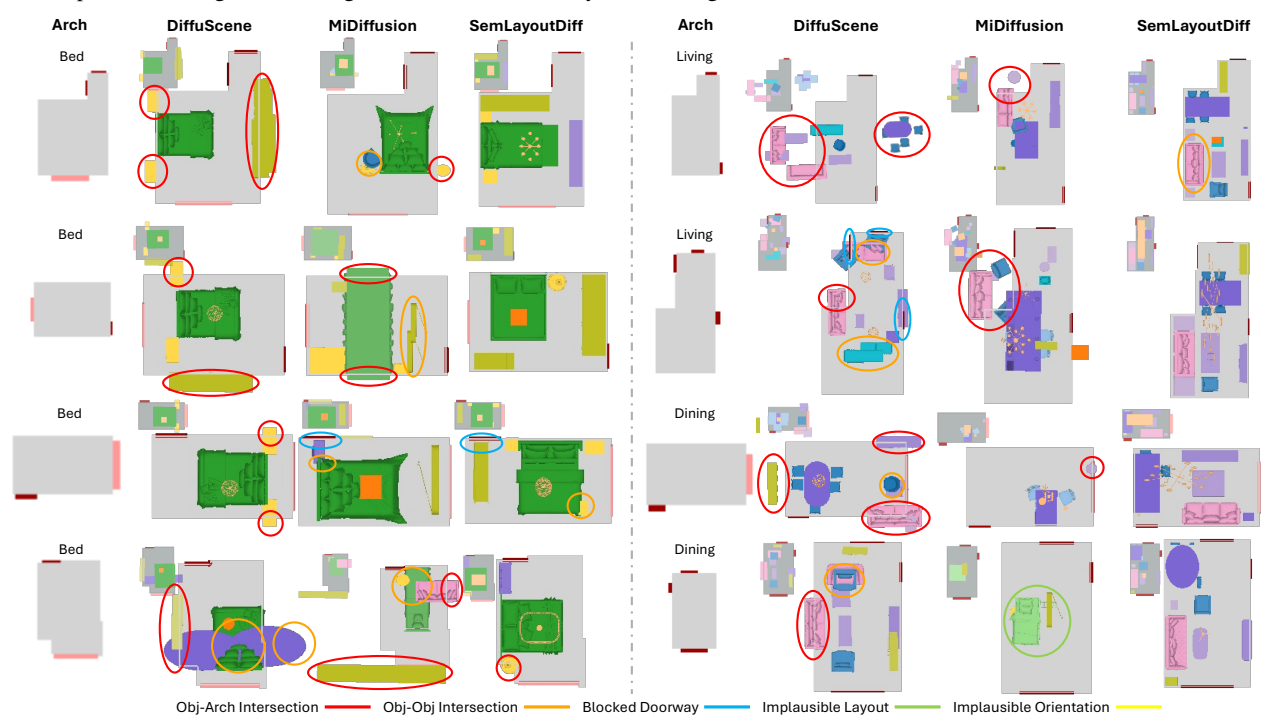


Figure 6. Comparison of generated scenes using different methods with *arch mask conditioning*. For each scene, we show the bounding box layout before object retrieval, inset on the upper left. Errors are indicated with color-coded circles (see Sec. 5.3 for error types). Our SEMLAYOUTDIFF generates scenes with fewer errors and respects architectural constraints by keeping furniture within room boundaries and maintaining clear spaces around doors (red) and windows (pink), whereas DIFFUSCENE and MIDIFFUSION do not.

lection of objects is severely limited, causing the SCA to easily identify generated scenes (see App. C.3). For the view-based metrics (KID, FID, SCA), we use a top-down semantic-colored rendering that clearly shows the objects and includes the architectural elements (see App. C.1).

To assess scene plausibility, we report the Out-of-Bounds (OOB) ratio [8] (ratio of objects placed outside

room boundaries). We report both the percentage of scenes (OOB_S) and the percentage of objects (OOB_O) with OOB issues. Finally, we report object collision rate (COL) and scene navigability (NAV) following SceneEval [38].

We report the performance of the different methods in Tabs. 1 and 2, where we see that our SEMLAYOUTDIFF consistently outperforms other unified methods.

Table 3. Comparison of different trainin	g strategies for SEMLAYOUTDIFF:	single condition (per-mas	ktype) vs mixed conditions.

			Distr	ibution		Plausibility					
Condition	Training	FID↓	KID↓	SCA%	CKL↓	$OOB_S \downarrow$	$OOB_O \downarrow$	COL↓	NAV↑		
None	per-masktype mixed	93.93 72.51	10.72 11.27	96.76 92.81	17.21 5.37	2.04 0.70	0.46 0.18	17.70 14.32	95.30 96.84		
Floor	per-masktype mixed	81.79 76.24	14.52 10.60	89.83 86.04	5.99 4.38	24.60 21.50	6.93 5.07	19.61 14.67	96.69 96.63		
Arch	per-roomtype per-masktype mixed	107.99 71.06 73.61	42.99 8.65 9.85	96.08 86.96 92.19	16.57 4.78 4.27	26.97 16.63 21.53	8.89 6.62 4.98	23.11 16.13 14.42	95.11 96.36 96.91		

Table 4. User rankings for the three methods on 40 samples.

		Rank Distribution						
Method	$AR\!\!\downarrow$	1st%	2nd $%$	3rd%				
DIFFUSCENE [39]	2.21	11.11	57.22	31.67				
MiDiffusion [16]	2.55	8.47	28.33	63.19				
SEMLAYOUTDIFF (Ours)	1.25	80.42	14.44	5.14				

Table 5. Fine-grained user evaluation. Users were asked to assess errors found in generated scenes.

	Interse	ection	Blocked	Implausible		
Method	Arch↓	Obj↓	Door↓	Layout↓	Orientation \downarrow	
DIFFUSCENE [39]	89.38	38.12	41.25	45.00	25.62	
MIDIFFUSION [16]	80.62	60.00	27.50	78.12	55.62	
SEMLAYOUTDIFF (Ours)	20.00	25.00	22.50	11.88	24.38	

SEMLAYOUTDIFF has a better distribution match to the ground-truth scenes. Compared to prior methods, SEMLAYOUTDIFF maintains closer visual and object distribution (see lower FID, KID, and CKL in Tab. 1). The other methods have unrealistic object distributions, such as placing beds in living rooms or dining tables in bedrooms (e.g., in Fig. 6, the MIDIFFUSION-generated dining room at the bottom right has a bed in the middle; the DIFFUSCENE-generated bedroom at the bottom left has two dining tables). This issue arises because these models are trained on a mixed object distribution across room types, which can confuse learning. In contrast, our model treats scene layout generation as a semantic image synthesis problem, conditioned specifically by room type, thus facilitating more effective learning of distinct object distributions.

Conditioning on floor and arch mask improves performance. Table 1 shows that adding conditioning on the floor or arch mask significantly improves scene synthesis. The overall FID for SEMLAYOUTDIFF drops from 93.93 for no room mask to 81.79 with floor conditioning and 71.06 for arch conditioning. The drop in FID, KID, and CKL shows that architecture information enables more realistic layouts matching the ground-truth distribution.

SEMLAYOUTDIFF better respects architectural constraints and generates more plausible layouts. Table 2 shows that our SEMLAYOUTDIFF consistently achieves

significantly lower scene-level (OOB_S) and object-level (OOB_O) out-of-boundary ratios compared to prior methods, across all room types. For instance, in bedrooms, SEM-LAYOUTDIFF reduces the OOB_S from approximately 55% (DIFFUSCENE) and 60% (MIDIFFUSION) to 13.8%, and the OOB_O from over 20% to only 4%. These results demonstrate our method's superior ability to place furniture objects accurately within architectural boundaries.

SEMLAYOUTDIFF also consistently has the lowest object-object collisions and maintains high navigability scores. For navigability, the only slight drop appears in bedrooms, where our navigability metric treats lights positioned below 2 meters as obstacles; such fixtures are common in practice, so this penalty does not reflect a real limitation of the layout. Overall, the results show that our method generates navigable layouts with less collisions.

Mixed-condition training. In our experiments so far, we have trained a separate model for each room mask type (none, floor, arch). We can also train one single unified model that can handle conditioning both on room type as well as different room mask types by training a single mixed condition model (see App. D.4 for details).

In Tab. 3, we show that with the mixed training, we generate scenes with slightly better distribution match and plausibility when conditioned on no room mask or just the floor mask. When conditioning on arch mask, the per-masktype model has slightly better distribution match. We also compare to training of a separate per-roomtype model. Notably, we find that per-roomtype training results in generated scenes that are further from the ground-truth distribution (high FID / KID / CKL) and poor plausibility (more out-of-bounds and collisions). The per-roomtype training suffers from both poor performance as well as the need for multiple models. By including all room types and mixing the conditioning allows the models to be trained on more data and learn the overall distribution better. To handle the different conditioning types, the per-roomtype training (as common in prior work) would need $M \times R$ separate models where R is the number of room-types and M is the number of mask types, vs M models for the per-masktype training, and 1 model for our proposed mixed condition training.

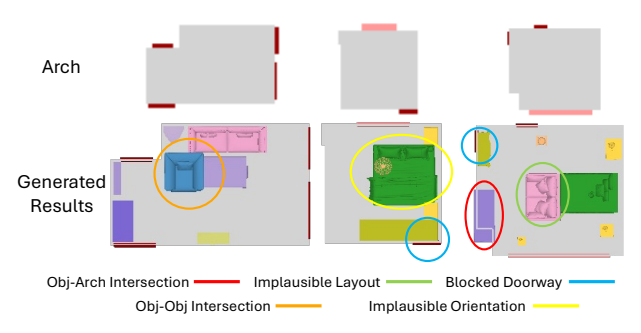


Figure 7. Examples of error cases for user study from SEMLAY-OUTDIFF-generated scenes with arch mask conditioning.

5.3. User study

To further compare the quality of the generated results, we conducted two user studies. As prior methods cannot generate the architecture, for fairer comparison we focus on generation conditioned on the arch mask. The first study asked participants to rank three generated scenes conditioned on the same architectural mask with different models according to plan adherence and overall layout plausibility. In Tab. 4, we report average ranking (AR) and the frequency of 1st, 2nd, and 3rd places. The second study examined five specific error types: object-architecture intersection or out-of-bounds, object-object intersection, blocked doorway, implausible layout, and implausible orientation (Fig. 7). We report the percentage of scenes in which each error appears (Tab. 5). See App. B.7 for more details on the user studies. **SEMLAYOUTDIFF** has the best performance. As shown in Tab. 4, SEMLAYOUTDIFF achieved the best average ranking (AR=1.25), with users selecting it as the best 80% of the time, and only 5% ranking it last. In the finegrained evaluation (Tab. 5), SEMLAYOUTDIFF also outperform DIFFUSCENE and MIDIFFUSION with users reporting lower issue rates in all 5 cases. Both user studies reinforces the findings from the automatic metrics: SEMLAYOUTDIFF generates the most plausible scenes as judged by people.

5.4. Discussion

Scene synthesis with generated object. In Fig. 8, we show that layouts from SEMLAYOUTDIFF can be converted into 3-D scenes by pairing them with a 3D object generation model. Specifically, we use TRELLIS [46], prompting it with "A <category>" to create a 3D object for each category in the layout. Then each mesh is scaled, translated, and rotated according to the predicted attributes.

Limitations. Despite the strong performance of our SEM-LAYOUTDIFF in unified indoor scene synthesis, it has several limitations. First, our method does not leverage object shape or contextual information, which could improve attribute predictions, such as orientation, and enhance object consistency. Second, SEMLAYOUTDIFF currently does not support conditioning on text or a partial scene, limiting the



Figure 8. Example of our synthesized scenes with TRELLIS-generated objects. Top left is the top-down rendering with 3D-FUTURE retrieved objects using our STK rendering, and bottom is the TRELLIS-based rendering with Blender.

level of user control. Third, relying on the small-scale 3D-FRONT dataset, which includes fewer than 5000 valid training rooms, constrains our model's potential; incorporating more diverse and extensive 2D and 3D scene data could enable the generation of more complex, multi-room layouts. Lastly, since our method uses top-down semantic maps, it struggles with vertical occlusion and hierarchical object arrangements. Future work can address this using a full 3D semantic voxel grid [48] or integrating semantic maps from multiple viewpoints, enabling better vertical layout generation.

6. Conclusion

In this work, we represent the indoor scene as the 2D semantic layout map with instance attributes to better capture the spatial relationship between objects and generalize to different room types. With this representation, we propose a novel indoor scene synthesis model called SEMLAYOUT-DIFF by leveraging the discrete denoising diffusion probabilistic model. Unlike most of the previous methods that are designed to train the models separately for different room types, our model is a unified model that can be generalized to different room types. Our model demonstrates flexibility in generation modes: it can operate without any room mask, with floor mask conditioning, or with full architectural mask conditioning. The ability to incorporate architectural elements (doors and windows) beyond just the floor mask is particularly valuable for indoor scene synthesis, as these elements impose important constraints on furniture placement and overall room layout. Compared to prior works, our approach exceeds the performance in unified room-type synthesis and can better place the objects in the conditioned room mask. Our proposed scene representation and corresponding method are important to the future of 3D generative modeling. We hope our work can inspire the following work to generate more complex and realistic scenes.

Acknowledgments

This work was funded in part by a CIFAR AI Chair and NSERC Discovery Grants, and enabled by support from the Digital Research Alliance of Canada and a CFI/BCKDF JELF. We thank Ivan Tam for help with running SceneEval; Yiming Zhang and Jiayi Liu for suggestions on figures; Derek Pun, Dongchen Yang, Xingguang Yan, and Manolis Savva for discussions, proofreading, and paper suggestions. We also thank the anonymous reviewers for their feedback.

References

- [1] Rio Aguina-Kang, Maxim Gumin, Do Heon Han, Stewart Morris, Seung Jean Yoo, Aditya Ganeshan, R Kenny Jones, Qiuhong Anna Wei, Kailiang Fu, and Daniel Ritchie. Open-universe indoor scene generation using LLM program synthesis and uncurated object databases. *arXiv preprint arXiv:2403.09675*, 2024. 1
- [2] Mikołaj Bińkowski, Danica J Sutherland, Michael Arbel, and Arthur Gretton. Demystifying MMD GANs. In *International Conference on Learning Representations*, 2018. 5
- [3] Ata Çelen, Guo Han, Konrad Schindler, Luc Van Gool, Iro Armeni, Anton Obukhov, and Xi Wang. I-design: Personalized LLM interior designer. arXiv preprint arXiv:2404.02838, 2024. 2
- [4] Shang Chai, Liansheng Zhuang, and Fengying Yan. LayoutDM: Transformer-based diffusion model for layout generation. In *Proceedings of the IEEE/CVF Conference on Computer Vision and Pattern Recognition*, pages 18349– 18358, 2023. 2
- [5] Dana Cohen-Bar, Elad Richardson, Gal Metzer, Raja Giryes, and Daniel Cohen-Or. Set-the-scene: Global-local training for generating controllable nerf scenes. *arXiv preprint arXiv:2303.13450*, 2023. 2
- [6] Matt Deitke, Eli VanderBilt, Alvaro Herrasti, Luca Weihs, Kiana Ehsani, Jordi Salvador, Winson Han, Eric Kolve, Aniruddha Kembhavi, and Roozbeh Mottaghi. ProcTHOR: Large-scale embodied AI using procedural generation. Advances in Neural Information Processing Systems, 35:5982–5994, 2022. 1
- [7] Maximilian Denninger, Dominik Winkelbauer, Martin Sundermeyer, Wout Boerdijk, Markus Wendelin Knauer, Klaus H Strobl, Matthias Humt, and Rudolph Triebel. BlenderProc2: A procedural pipeline for photorealistic rendering. *Journal of Open Source Software*, 8(82):4901, 2023. 3, 12
- [8] Weixi Feng, Wanrong Zhu, Tsu-jui Fu, Varun Jampani, Ar-jun Akula, Xuehai He, Sugato Basu, Xin Eric Wang, and William Yang Wang. LayoutGPT: Compositional visual planning and generation with large language models. arXiv preprint arXiv:2305.15393, 2023. 6, 17, 18
- [9] Matthew Fisher, Daniel Ritchie, Manolis Savva, Thomas Funkhouser, and Pat Hanrahan. Example-based synthesis of 3D object arrangements. ACM Transactions on Graphics (TOG), 31(6):1–11, 2012. 1, 2
- [10] Huan Fu, Bowen Cai, Lin Gao, Ling-Xiao Zhang, Jiaming Wang, Cao Li, Qixun Zeng, Chengyue Sun, Rongfei Jia,

- Binqiang Zhao, et al. 3D-Front: 3D furnished rooms with layouts and semantics. In *Proceedings of the IEEE/CVF International Conference on Computer Vision*, pages 10933–10942, 2021. 2, 4
- [11] Gege Gao, Weiyang Liu, Anpei Chen, Andreas Geiger, and Bernhard Schölkopf. GraphDreamer: Compositional 3D scene synthesis from scene graphs, 2023. 2
- [12] Lin Gao, Jia-Mu Sun, Kaichun Mo, Yu-Kun Lai, Leonidas J Guibas, and Jie Yang. SceneHGN: Hierarchical graph networks for 3D indoor scene generation with fine-grained geometry. *IEEE Transactions on Pattern Analysis and Machine Intelligence*, 45(7):8902–8919, 2023. 2
- [13] Martin Heusel, Hubert Ramsauer, Thomas Unterthiner, Bernhard Nessler, and Sepp Hochreiter. GANs trained by a two time-scale update rule converge to a local Nash equilibrium. Advances in neural information processing systems, 30, 2017. 5
- [14] Jonathan Ho, Ajay Jain, and Pieter Abbeel. Denoising diffusion probabilistic models. Advances in Neural Information Processing Systems, 33:6840–6851, 2020. 2
- [15] Emiel Hoogeboom, Didrik Nielsen, Priyank Jaini, Patrick Forré, and Max Welling. Argmax flows and multinomial diffusion: Learning categorical distributions. Advances in Neural Information Processing Systems, 34:12454–12465, 2021. 2, 3
- [16] Siyi Hu, Diego Martin Arroyo, Stephanie Debats, Fabian Manhardt, Luca Carlone, and Federico Tombari. Mixed diffusion for 3D indoor scene synthesis. arXiv preprint arXiv:2405.21066, 2024. 1, 2, 3, 4, 5, 7, 13, 15, 20, 21, 22, 23
- [17] Ziniu Hu, Ahmet Iscen, Aashi Jain, Thomas Kipf, Yisong Yue, David A Ross, Cordelia Schmid, and Alireza Fathi. SceneCraft: An LLM agent for synthesizing 3D scene as Blender code. In *ICLR 2024 Workshop on Large Language Model (LLM) Agents*, 2024. 2
- [18] Naoto Inoue, Kotaro Kikuchi, Edgar Simo-Serra, Mayu Otani, and Kota Yamaguchi. LayoutDM: Discrete diffusion model for controllable layout generation. In *Proceedings of the IEEE/CVF Conference on Computer Vision and Pattern Recognition*, pages 10167–10176, 2023. 2
- [19] Diederik P. Kingma and Jimmy Ba. Adam: A method for stochastic optimization. In *International Conference on Learning Representations*, 2015. 13
- [20] Manyi Li, Akshay Gadi Patil, Kai Xu, Siddhartha Chaudhuri, Owais Khan, Ariel Shamir, Changhe Tu, Baoquan Chen, Daniel Cohen-Or, and Hao Zhang. GRAINS: Generative recursive autoencoders for indoor scenes. ACM Transactions on Graphics (TOG), 38(2):1–16, 2019.
- [21] Chenguo Lin and Yadong Mu. InstructScene: Instruction-driven 3D indoor scene synthesis with semantic graph prior. In *International Conference on Learning Representations*, 2024. 2
- [22] Yiqi Lin, Haotian Bai, Sijia Li, Haonan Lu, Xiaodong Lin, Hui Xiong, and Lin Wang. CompoNeRF: Text-guided multi-object compositional nerf with editable 3D scene layout. arXiv preprint arXiv:2303.13843, 2023. 2
- [23] Andrew Luo, Zhoutong Zhang, Jiajun Wu, and Joshua B Tenenbaum. End-to-end optimization of scene layout. In

- Proceedings of the IEEE/CVF Conference on Computer Vision and Pattern Recognition, pages 3754–3763, 2020. 2
- [24] Léopold Maillard, Nicolas Sereyjol-Garros, Tom Durand, and Maks Ovsjanikov. DeBaRA: Denoising-based 3D room arrangement generation. Advances in Neural Information Processing Systems, 2024. 2
- [25] Paul Merrell, Eric Schkufza, Zeyang Li, Maneesh Agrawala, and Vladlen Koltun. Interactive furniture layout using interior design guidelines. ACM transactions on graphics (TOG), 30(4):1–10, 2011. 1, 2
- [26] Wamiq Reyaz Para, Paul Guerrero, Niloy Mitra, and Peter Wonka. COFS: Controllable furniture layout synthesis. In ACM SIGGRAPH Conference Proceedings, 2023. 2
- [27] Despoina Paschalidou, Amlan Kar, Maria Shugrina, Karsten Kreis, Andreas Geiger, and Sanja Fidler. ATISS: Autoregressive transformers for indoor scene synthesis. *Advances in Neural Information Processing Systems*, 34:12013–12026, 2021. 1, 2, 3, 4, 5, 12, 13, 15, 17, 18, 21
- [28] Ryan Po and Gordon Wetzstein. Compositional 3D scene generation using locally conditioned diffusion. arXiv preprint arXiv:2303.12218, 2023.
- [29] Alexander Raistrick, Lahav Lipson, Zeyu Ma, Lingjie Mei, Mingzhe Wang, Yiming Zuo, Karhan Kayan, Hongyu Wen, Beining Han, Yihan Wang, Alejandro Newell, Hei Law, Ankit Goyal, Kaiyu Yang, and Jia Deng. Infinite photorealistic worlds using procedural generation. In Proceedings of the IEEE/CVF Conference on Computer Vision and Pattern Recognition, pages 12630–12641, 2023.
- [30] Daniel Ritchie, Kai Wang, and Yu-an Lin. Fast and flexible indoor scene synthesis via deep convolutional generative models. In *Proceedings of the IEEE/CVF Conference on Computer Vision and Pattern Recognition*, pages 6182–6190, 2019. 2
- [31] Jascha Sohl-Dickstein, Eric Weiss, Niru Maheswaranathan, and Surya Ganguli. Deep unsupervised learning using nonequilibrium thermodynamics. In *International Conference on Machine Learning*, pages 2256–2265. PMLR, 2015.
- [32] Jiaming Song, Chenlin Meng, and Stefano Ermon. Denoising diffusion implicit models. In *International Conference on Learning Representations*, 2021.
- [33] Yang Song and Stefano Ermon. Improved techniques for training score-based generative models. Advances in neural information processing systems, 33:12438–12448, 2020. 2
- [34] Chong Su, Yingbin Fu, Zheyuan Hu, Jing Yang, Param Hanji, Shaojun Wang, Xuan Zhao, Cengiz Öztireli, and Fangcheng Zhong. CHOrD: Generation of collision-free, house-scale, and organized digital twins for 3D indoor scenes with controllable floor plans and optimal layouts. *arXiv preprint arXiv:2503.11958*, 2025. 2, 4
- [35] Fan-Yun Sun, Weiyu Liu, Siyi Gu, Dylan Lim, Goutam Bhat, Federico Tombari, Manling Li, Nick Haber, and Jiajun Wu. LayoutVLM: Differentiable optimization of 3D layout via vision-language models. arXiv preprint arXiv:2412.02193, 2024.
- [36] Kaifan Sun, Bingchen Yang, Peter Wonka, Jun Xiao, and Haiyong Jiang. RelTriple: Learning plausible indoor layouts

- by integrating relationship triples into the diffusion process. *arXiv preprint arXiv:2503.20289*, 2025. 2
- [37] Qi Sun, Hang Zhou, Wengang Zhou, Li Li, and Houqiang Li. Forest2Seq: Revitalizing order prior for sequential indoor scene synthesis. In *European Conference on Computer Vision*, 2024. 2
- [38] Hou In Ivan Tam, Hou In Derek Pun, Austin T Wang, Angel X Chang, and Manolis Savva. SceneEval: Evaluating semantic coherence in text-conditioned 3D indoor scene synthesis. *arXiv* preprint arXiv:2503.14756, 2025. 6, 13
- [39] Jiapeng Tang, Yinyu Nie, Lev Markhasin, Angela Dai, Justus Thies, and Matthias Nießner. DiffuScene: Scene graph denoising diffusion probabilistic model for generative indoor scene synthesis. *arXiv preprint arXiv:2303.14207*, 2023. 1, 2, 3, 4, 5, 7, 12, 13, 15, 16, 17, 18, 20, 21, 22, 23
- [40] Alexander Vilesov, Pradyumna Chari, and Achuta Kadambi. CG3D: Compositional generation for text-to-3D via gaussian splatting. arXiv preprint arXiv:2311.17907, 2023. 2
- [41] Kai Wang, Manolis Savva, Angel X Chang, and Daniel Ritchie. Deep convolutional priors for indoor scene synthesis. ACM Transactions on Graphics (TOG), 37(4):1–14, 2018. 1, 2
- [42] Kai Wang, Yu-An Lin, Ben Weissmann, Manolis Savva, Angel X Chang, and Daniel Ritchie. PlanIT: Planning and instantiating indoor scenes with relation graph and spatial prior networks. ACM Transactions on Graphics (TOG), 38(4):1–15, 2019. 1, 2
- [43] Xinpeng Wang, Chandan Yeshwanth, and Matthias Nießner. Sceneformer: Indoor scene generation with transformers. In 2021 International Conference on 3D Vision (3DV), pages 106–115. IEEE, 2021. 1, 2
- [44] Qiuhong Anna Wei, Sijie Ding, Jeong Joon Park, Rahul Sajnani, Adrien Poulenard, Srinath Sridhar, and Leonidas Guibas. Lego-net: Learning regular rearrangements of objects in rooms. In Proceedings of the IEEE/CVF Conference on Computer Vision and Pattern Recognition, pages 19037–19047, 2023. 13
- [45] Zehao Wen, Zichen Liu, Srinath Sridhar, and Rao Fu. Any-Home: Open-vocabulary generation of structured and textured 3D homes. arXiv preprint arXiv:2312.06644, 2023. 2
- [46] Jianfeng Xiang, Zelong Lv, Sicheng Xu, Yu Deng, Ruicheng Wang, Bowen Zhang, Dong Chen, Xin Tong, and Jiaolong Yang. Structured 3D latents for scalable and versatile 3D generation. In *IEEE Conference on Computer Vision and Pattern Recognition*, 2025. 8
- [47] Ken Xu, James Stewart, and Eugene Fiume. Constraint-based automatic placement for scene composition. In *Graphics Interface*, pages 25–34, 2002. 2
- [48] Ming-Jia Yang, Yu-Xiao Guo, Bin Zhou, and Xin Tong. Indoor scene generation from a collection of semanticsegmented depth images. In *Proceedings of the IEEE/CVF International Conference on Computer Vision*, pages 15203– 15212, 2021. 8
- [49] Yandan Yang, Baoxiong Jia, Peiyuan Zhi, and Siyuan Huang. PhyScene: Physically interactable 3D scene synthesis for embodied AI. In Proceedings of the IEEE/CVF Conference on Computer Vision and Pattern Recognition, pages 16262–16272, 2024. 2, 5, 23

- [50] Yue Yang, Fan-Yun Sun, Luca Weihs, Eli VanderBilt, Alvaro Herrasti, Winson Han, Jiajun Wu, Nick Haber, Ranjay Krishna, Lingjie Liu, et al. Holodeck: Language guided generation of 3D embodied AI environments. In *IEEE Conference* on Computer Vision and Pattern Recognition, pages 20–25. IEEE/CVF, 2024. 2
- [51] Guangyao Zhai, Evin Pinar Örnek, Shun-Cheng Wu, Yan Di, Federico Tombari, Nassir Navab, and Benjamin Busam. CommonScenes: Generating commonsense 3D indoor scenes with scene graphs. Advances in Neural Information Processing Systems, 2023. 2
- [52] Guangyao Zhai, Evin Pınar Örnek, Dave Zhenyu Chen, Ruotong Liao, Yan Di, Nassir Navab, Federico Tombari, and Benjamin Busam. Echoscene: Indoor scene generation via information echo over scene graph diffusion. In *European Conference on Computer Vision*, pages 167–184. Springer, 2024. 2
- [53] Zaiwei Zhang, Zhenpei Yang, Chongyang Ma, Linjie Luo, Alexander Huth, Etienne Vouga, and Qixing Huang. Deep generative modeling for scene synthesis via hybrid representations. ACM Transactions on Graphics (TOG), 39(2):1–21, 2020. 2
- [54] Yang Zhou, Zachary While, and Evangelos Kalogerakis. SceneGraphNet: Neural message passing for 3D indoor scene augmentation. In *Proceedings of the IEEE/CVF Inter*national Conference on Computer Vision, pages 7384–7392, 2019. 2

SemLayoutDiff: Semantic Layout Generation with Diffusion Model for Indoor Scene Synthesis

Supplementary Material

In this supplement, we present model details (App. A), additional information about our experimental setup (App. B), preliminary experiments to investigate the impact of rendering changes to evaluation metrics (App. C), and additional results (App. D).

A. Model details

Instance extraction. Given the semantic map, we extract instances by finding connected components (with horizontal and vertical grid cells as neighbors) and identifying each connected region with the same category label as an individual object instance. Specifically, we use the *label* function in *scipy* library to process the binary mask for each category. **Object retrieval.** For each extracted object instance, we retrieve a corresponding 3D model from a subset of 3D-FUTURE assets, which are used in the filtered rooms, by computing the mean squared error (MSE) between the predicted 3D size of the instance and the sizes of available assets within the same category. The asset with the lowest MSE is selected as the best match:

$$\mathbf{a}^* = \arg\min_{\mathbf{a} \in \mathcal{A}_c} \mathrm{MSE}(\mathbf{s}_p, \mathbf{s}_a)$$

where

$$MSE(\mathbf{s}_{p}, \mathbf{s}_{a}) = \frac{1}{3} \sum_{d \in \{x, y, z\}} (s_{p, d} - s_{a, d})^{2},$$

and s_p and s_a denote the predicted and candidate asset sizes respectively, and A_c is the set of assets for category c.

Room construction. Based on the generated semantic map, we extract the outline of the floor for two cases: (1) For floor- or architecture-conditioned generation, we directly use the floor or architecture mask, mapping each pixel to real-world coordinates on the xy-plane at a height of 0, with each pixel representing 0.01 meters. (2) For unconditional generation, we treat all non-zero pixels as floor, and similarly, extract the positions of doors and windows from their respective mask regions. We assume that doors are 2 meters tall and windows are rectangular, with a vertical offset of 0.5 meters to 2 meters. We construct the 3D geometry of the room by taking the room outline and creating planar walls, assuming a wall height of 3 meters, and cutting out rectangular holes for the doors and windows.

B. Experimental details

We provide details on our experimental setup, including the data preprocessing and filtering (App. B.1) for our experi-

ments, the unified set of object categories (App. B.2), how baseline models are adapted and trained (App. B.3), training details for our SEMLAYOUTDIFF (App. B.4), discussion of compute and memory cost (App. B.5), evaluation metric details (App. B.6), and details of our user study (App. B.7).

B.1. Data processing

We preprocess the data and use BlenderProc [7], to render top-down views of the scenes. For the semantic scene layout, we render both instance and semantic masks. We follow the steps below for processing the data:

- 1. We first extract rooms from scenes based on their room types (e.g. bedroom, living room, dining room) and filter the data following DiffuScene [39]. Specifically, we remove rooms with unnatural dimensions (e.g., overly large sizes or extreme heights), discard infrequent objects appearing in fewer than 15 rooms, and exclude scenes containing overlapping or misplaced objects, as well as rooms with an insufficient or excessive number of objects.
- 2. After this filtering process, the dataset includes 4041 bedrooms, 900 living rooms, and 813 dining rooms. For the unified dataset, we combine all room types and split the processed data into 70% training, 10% validation, and 20% test following prior work [27, 39].
- 3. We render the top-down 2D semantic layout map using orthographic projection, where the camera is positioned at the center top of the room. To ensure that each pixel on the map represents a consistent physical unit s, we compute the desired image dimensions in pixels $(w_{\rm img}, h_{\rm img})$ from the input room width $w_{\rm room}$ and length $l_{\rm room}$ in meters. As we render a top-down view, the image dimensions are given by: $(w_{\rm img}, h_{\rm img}) = (w_{\rm room}, l_{\rm room})/s$. We set the Blender orthographic scale $(OS)^1$ to the maximum of the room width and length $(OS = \max(w_{\rm room}, l_{\rm room}))$. We pad the image to 1200×1200 (corresponding to $12 \, {\rm m} \times 12 \, {\rm m}$) for later training and inference.
- 4. We then extract the objects' category, size, vertical position (offset from floor), and orientation based on the annotations. The offset is determined by measuring the maximum distance from the object's bounding box to the floor.

¹The Blender orthographic scale specifies the larger dimension in scene units (meters)

B.2. Unified object categories

We use the same object categories following ATISS and DiffuScene. In those works, different sets of object categories were used for different room types. To obtain a unified set of object categories, we combine object types from different room types into a single unified set. To ensure clarity regarding the object categories used in our analysis, we provide a list of the unified categories as follows: kids bed, single bed, double bed, corner side table, round end table, coffee table, console table, tv stand, desk, dressing table, table, dining table, stool, dressing chair, dining chair, chinese chair, armchair, chair, lounge chair, loveseat sofa, lazy sofa, sofa, multi seat sofa, chaise longue sofa, 1 shaped sofa, nightstand, shelf, bookshelf, children cabinet, wine cabinet, cabinet, wardrobe, pendant lamp, ceiling lamp, floor, door, window, void.

B.3. Adapting prior methods

For fair comparison, we adapt DIFFUSCENE and MIDIFFUSION to train unified models that handle all room types, instead of their original separate models per room type. We modify these methods to accept both architecture plan and room type as conditioning inputs. To allow conditioning by room type, we adapt the models so that the room type is passed in as a one-hot vector and then converted into a dense representation using a Multi-Layer Perceptron (MLP). We also modified DIFFUSCENE and MIDIFFUSION to incorporate architectural plan conditioning. **DIFFUSCENE** [39] represents scenes as fully connected graphs, with each node corresponding to an object and its attributes. It also uses dense representations for room type and floorplan as instance-level attributes, supplemented with positional encodings to position objects accurately.

During inference, this ensures the generation of coherent scenes aligned with the provided floorplan and room type. Without floor conditioning, the floorplan vector is omitted during training. To adapt this method, we represent the architectural plan $\mathcal A$ as a single-channel image and extract architecture features using a ResNet-18 encoder.

MIDIFFUSION [16] represents scenes as sequences of objects with attributes, similar to ATISS and DIFFUSCENE. However, it treats object attributes as both discrete (object categories) and continuous (size, orientation, position). MIDIFFUSION incorporates additional spatial information by representing the floor as a set of 2D points with normals, following the approach described in [44]. It employs a PointNet encoder, trained from scratch, to extract features from the floormask. To incorporate architectural constraints, we extract points and normals from the architecture

Table 6. Compute and memory cost of different models

		Train	Infere	ence
	Time	Mem	Time	Mem
DIFFUSCENE	52h	5G (batch=128)	25.0s	0.5G
MIDIFFUSION	120h	4G (batch=128)	11.0s	0.4G
SEMLAYOUTDIFF	60h	11G (batch=24)	18.2s	1.4G

mask separately, including floor, door, and window information. We encode the door and window features using a PointNet encoder and sum these features together. The summed feature is then concatenated with the floormask feature obtained from the original MIDIFFUSION approach to form the architecture conditioning feature for the model.

B.4. SEMLAYOUTDIFF **Training details**

Semantic Layout Generation. We train the diffusion model using the Adam optimizer [19] with 4000 diffusion steps and a batch size of 64. We use a constant learning rate of 1e-4. Training was conducted on a single 48G A40 GPU over 1000 epochs, completed in 24 hours.

Attribute Prediction Module. We train the APM using the Adam optimizer [19] with a weight decay of 1e-3 and a learning rate of 1e-5. The model processed images at a resolution of 1200×1200 using a batch size of 24. Training was conducted on a single 48G A40 GPU for 300 epochs, taking \sim 36 hours.

B.5. Model efficiency

Under the architecture-mask conditioning and unified setting, SEMLAYOUTDIFF samples a room in 18.2 seconds: 18s for the 4,000 diffusion steps and 0.2s for attribute prediction. Its semantic layout map and attribute models are trained in 24h and 36h, respectively; trained in parallel, the wall-clock time is 36h. MIDIFFUSION needs 11s per scene with a 1,000-step schedule but 120h for training. DIFFUSCENE spends 25s per scene with the same 1,000 steps and trains in 52h. Hence, SEMLAYOUTDIFF attains moderate inference latency and a lower training time than MIDIFFUSION. See Tab. 6 for a summary.

B.6. Evaluation metric details

To assess the quality of generated scenes, we use a set of quantitative metrics that cover visual fidelity, semantic consistency, category distribution, spatial plausibility, and navigability. Following prior work [27, 39], we adopt FID, KID, and SCA for image-based evaluation and CKL for measuring the category distribution alignment. From SceneEval [38], we adopt COL to assess object-level collisions and NAV to evaluate scene navigability. In addition, we implement our own OOB-scene and OOB-object metrics to check whether objects extend beyond the floor boundary.

Indoor Scene Generation User Study

Thank you for participating in our survey on indoor scene generation.

In this study, you will be shown an **architectural plan** (the "condition") along with **three different generated indoor scenes**. We would like you to evaluate these scenes based on **Architecture Layout Fidelity and Object Arrangement**:

Architecture Layout Fidelity

- Do the objects in the generated scene align correctly within the provided plan?
- Are any doors (in red) or windows (in pink) blocked by objects?

Object Arrangement

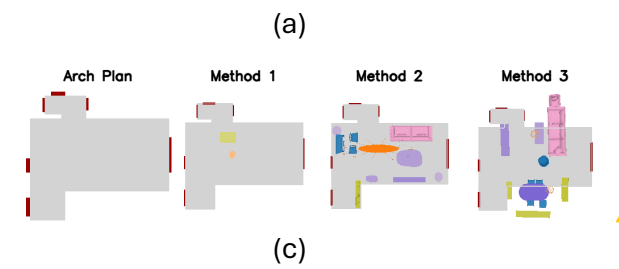
• Do the orientation, position, and scale of the objects make sense?

How the survey works:

- For each question, you will see 4 images: the architecture plan (condition) and three top-down renderings of generated scenes from different methods.
- The objects in these renderings are color-coded by their semantic labels, and each scene is shown from an orthographic top-down view.
- Please rank the three generated scenes from best to worst based on the above criteria.
- Note that the orange color means pendant lamp, which is fine to intersect with othe objects in top-down view of the room.

▲ In cases where it's difficult to decide, **prioritize Architecture Layout Fidelity** over Object Arrangement.

Thank you for your time and thoughtful responses!



Detailed evaluation of indoor scene synthesis

Thank you for participating in our survey on indoor scene generation.

In this study, you will be shown an architectural plan (the "condition") along with three different generated indoor scenes. We would like you to evaluate these scenes across different aspects:

- Object-architecture intersection: Check if any furniture or objects are overlapping
 with architectural elements like walls, windows, or doors. Or if any object is out of
 the room boundary.
- Object-object intersection: Check if any objects are intersecting or overlapping with
 each other in unrealistic ways. For example, it is OK for the chairs to have some
 overlap with the table from the top-down view. But it is not acceptable if the chairs
 overlap with bed or wardrobe.
- Blocking doorways: Check if any objects are placed in a way that blocks access to doorways or impedes movement between rooms.
- Implausible layout: Check if the overall arrangement of objects in the room is unrealistic or unconventional (e.g., bed in front of the stove).
- Implausible orientation: Check if any objects are facing the wrong direction or rotated in a way that makes their use impractical.

How the survey works:

- For each question, you will see 4 images: the architecture plan (condition) and three top-down renderings of generated scenes from different methods.
- The objects in these renderings are color-coded by their semantic labels, and each scene is shown from an **orthographic top-down view**.
- Please Evaluate each of the three generated scenes for each example across all the evaluation aspects listed above. Check the box if a scene exhibits the corresponding issue.
- Note that the orange color means pendant lamp, which is fine to intersect with other objects in top-down view of the room
- Below is the color palette for different object categories. You can refer to it to help you evalute the object arrangement. For simplicity, similar object types is shown in similar colors. For example, greenish objects represent beds
- If none of the methods has the specific issue, choose None for that corresponding box.

You should evaluate each method results for each evaluation critiria

(b)

Figure B.1. User study details. (a) shows the detailed instruction of our overall quality evaluation user study; (b) shows the detailed instruction of our fine-grained user study to evaluate specific error types in the generated rooms; (c) shows an example of the provided sample, including arch plan and randomly ordered generated rooms from three different methods.

Together, these metrics provide a complementary and thorough evaluation of scene generation quality.

FID and KID. Fréchet Inception Distance (FID) and Kernel Inception Distance (KID) are standard image generation evaluation metrics for measuring how well the generated images match the distribution of the training images. For scene generation, rendered images are typically used. FID computes the distance between Gaussian distributions fitted on features of generated and real images:

$$FID = \|\mu_r - \mu_g\|_2^2 + Tr\left(\Sigma_r + \Sigma_g - 2(\Sigma_r \Sigma_g)^{1/2}\right),$$

where (μ_r, Σ_r) and (μ_g, Σ_g) are the mean and covariance of real and generated features. KID instead uses the squared Maximum Mean Discrepancy (MMD) with a polynomial kernel:

$$KID = \mathbb{E}[k(x_r, x_r')] + \mathbb{E}[k(x_g, x_g')] - 2\mathbb{E}[k(x_r, x_g)],$$

where k is a polynomial kernel and expectations are taken over real (x_r) and generated (x_q) features.

SCA. Scene classifier accuracy (SCA) measures whether generated images preserve semantic consistency, by clas-

sifying each generated scene image into a room type and reporting the classification accuracy. For the SCA classifier, the classifier is trained for each set of generated scenes. The classifier is trained to distinguish the ground truth training scenes from 500 different synthesized scenes (half of 1000). The trained classifier is then evaluated on the other 500 synthesized scenes and the ground truth test scenes.

CKL. Category KL divergence (CKL) evaluates the alignment of category distributions between generated and real scenes. Let p(c) and q(c) be the normalized category frequencies (GT and generated). We compute:

CKL =
$$\sum_{c} p(c) \log \frac{p(c) + \varepsilon}{q(c) + \varepsilon}$$
, $\varepsilon = 10^{-6}$.

A lower value indicates that the generated scenes reproduce the real-world category frequency more faithfully.

OOB-scene and OOB-object. The out-of-boundary (OOB) metrics detect objects that extend beyond the floor boundary based on their 3D bounding boxes. An object is marked OOB if any part lies outside the floor polygon. OOB-object reports the ratio of such objects over all ob-

Table 7. Sanity checks for DIFFUSCENE under the condition that uses DIFFUSCENE semantic class-based rendering and w/o floor. We compare our retrained model against that of the results reported in the original paper.

	Bedroom					Dinir	ng room		Living room			
Method	FID↓	KID↓	SCA%	CKL↓	FID↓	KID↓	SCA%	CKL↓	FID↓	KID↓	SCA%	CKL↓
DIFFUSCENE (paper)	17.21	0.7	53.52	0.35	32.60	0.72	55.50	0.22	36.18	0.88	57.81	0.21
DIFFUSCENE (pretrained)	26.66	2.77	63.03	0.39	30.85	4.94	60.32	0.28	27.95	3.30	54.89	0.31
DIFFUSCENE (retrained)	28.18	0.19	53.33	0.41	41.49	0.60	50.07	0.27	43.37	0.46	53.88	0.44

jects, while OOB-scene reports the ratio of scenes that contain at least one OOB object. These metrics capture violations of spatial plausibility.

COL. Collisions (COL) evaluates whether objects in a scene physically intersect with each other. We perform pairwise mesh-level intersection tests among all objects, and count the percentage of objects involved in any collision. A lower COL indicates that the generated layout respects basic physical plausibility.

NAV. Navigability (NAV) measures how easily an agent can move through the scene. We project the scene onto the floor plane, mask out the regions occupied by objects, and compute the largest connected free space. The ratio of this largest region to the total free space indicates navigability. A higher NAV means the layout allows smooth movement and avoids isolated or blocked areas.

B.7. User study details

We conduct two separate user studies: a) an overall assessment of scene quality and b) a more fine-grained evaluation of errors in the generated scenes. In Fig. B.1 (a,b), we show the full instructions we provided the users for the two studies. For each study, we show the partipants generated scenes from the three methods (the baseline methods DiffuScene and MiDiffusion, and our SemLayoutDiff) with a random ordering of the methods, and the method names hidden to prevent bias. We show the input architectural plan and the semantic coloured, top-down scenes generated by each of the three methods in random order (Fig. B.1 (c)). We used the same 40 arch + scenes for the two studies. We recruited 18 participants to conduct the overall quality evaluation study and 4 participants for the second fine-grained evaluation study.

Overall quality evaluation. Participants ranked the scenes 1 (best) to 3 (worst) based on the overall quality. If the quality is hard to rank, the participants first judged how well each method's result fits in the architecture plan; then they compared overall object arrangement (Fig. B.1 (a)).

Fine-grained evaluation. For this study, participants used a grid of checkboxes to indicate what errors were present for each scene. We asked users to assess whether the scene had any of the following five types of errors: object architecture overlap, object object overlap, blocked doorway, im-

plausible layout, and wrong orientation. Note that object architecture overlap also includes cases where an object is placed entirely outside the wall boundary. Participants were asked to select every issue they detected for each scene or chose "none" if none applied (Fig. B.1 (b)).

C. Preliminary experiments

For our experiments, we use a modified color palette and rendering setup differing from prior work [16, 27, 39]. Our modified palette (Fig. C.3) was selected to be a single palette that included all object categories across the different room types, and used similar colors for closely related object categories (e.g. greens for the different beds – kids bed, single bed, double bed). For rendering, we developed our own tool to render an arbitrarily shaped room layout with architecture information (e.g. showing the placement of windows and doors).

We render with a flatter shading, whereas earlier work used a camera-mounted point light in simple3dviz. Compared with prior work, we also render with a more zoomedin view that allows for closer inspection of the object details. Figure C.2 shows examples comparing renderings using our rendering tool (STK) and our new color palette and those using simple3dviz with the color palette used by DiffuScene and prior work. Figure C.3 shows the differences in color palettes between prior work (left two) and ours (right). Our color palette assigns similar colors to object categories with similar functions. We conduct a series of experiments to account for how changes in rendering styles impact the common evaluation metrics used in scene generation. We first conduct initial sanity experiments on DiffuScene [39] (App. C.1), to set a point of comparison for our studies on the impact of changes in renderings (App. C.2).

C.1. Reproducing prior work results

We used the pretrained DIFFUSCENE weights for the sanity check. The training is on a single A40 GPU with a batch size of 128 for 100k epochs. We set the learning rate $l_T=2e^{-4}$ with a decay rate of 0.5 in every 15k epochs. The noise intensity linearly increases from 0.0001 to 0.02 with 1000 time steps. The above settings exactly follow the original implementation of DIFFUSCENE. However, from Table 7, the pretrained results are not as good as reported

	Bedroom	Bedroom	Dining room	Living room
simple3dviz (original palette, overhead point-light)		<u>.</u>		
STK (new palette, constant illumination)				
STK (with architecture)				

Figure C.2. Examples of top-down renderings using simple3dviz with original palette (top), STK with updated palette (mid), STK with updated palette and actual architecture (bottom). In our new color palette (see Fig. C.3), we use similar colors for similar object categories (e.g. single_bed vs double_bed), resulting in more consistent coloring of objects across rooms (e.g. different types of sofa are colored similarly) with semantically different types of objects being more distinct (e.g. chairs around tables in column 3 are more sharply contrasted in the bottom row vs the top). We also eliminate the point light, and visualize the actual architectural elements (floor, door, window). These rendering changes aims to eliminate the lighting effect, and focus on the semantics of the objects and their placement with respect to the architecture elements.

Table 8. Comparison of how metrics change with different styles for DiffuScene (with simple-3dviz, unconditioned).

		Bedroom			Dining room			Living room		
Coloring (palette)	Floor	FID↓	KID↓	SCA%	FID↓	KID↓	SCA%	FID↓	KID↓	SCA%
Semantic (DiffuScene)	none	26.66	2.77	63.03	30.85	4.94	60.32	27.95	3.30	54.89
Semantic (ours)	none	27.32	2.99	71.02	35.23	5.93	58.39	32.12	4.17	55.71
Semantic (DiffuScene)	square	32.98	0.49	54.16	45.79	0.86	49.37	45.37	0.81	51.67
Semantic (ours)	square	34.52	1.12	58.01	49.69	0.51	49.86	50.10	0.45	53.41
Textured	square	46.55	0.34	50.43	63.03	0.39	44.43	60.27	0.47	48.75

in the paper [39]. We also tried to retrain the DiffuScene model to follow the DiffuScene instruction and setting exactly. We find that both the retrained and pretrained models perform worse than the reported results in the paper.

To confirm that our DiffuScene model is trained well, we use a rendering similar to the one used in the original paper (semantic class-based rendering without floor) and compare the results with those reported in the paper (Ta-

ble 7). We find that our retrained model has better KID and SCA than reported in the paper, but slightly worse FID and CKL. Via correspondence with the authors, we confirmed that some deviation from the reported numbers in the paper is expected when retraining.

C.2. Impact of rendering style on metrics

We note that the metrics are strongly influenced by rendering style, including whether a floor is included in the ren-

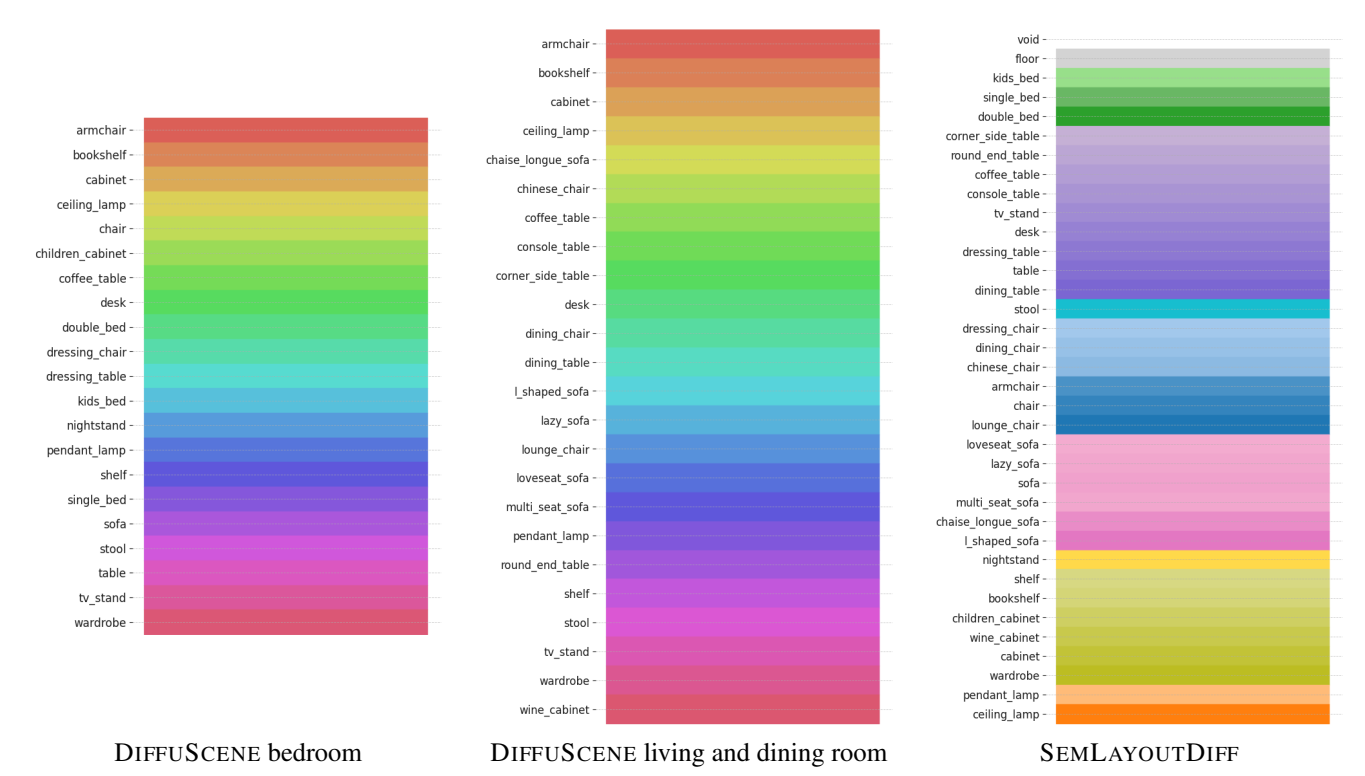


Figure C.3. The original color palette used by DiffuScene [39] vs the unified color palette that we use for rendering semantic colored scenes for evaluation. Compared to the original color paletted, we tried to use similar colors for semantic classes that were more similar to each other. For instance, we used shades of orange for both pendant_lamp and ceiling_lamp and shades of purple for various types of tables. In addition, we tried to ensure classes that are semantically more different used more distinct colors (e.g. we used blue for chairs vs very close shades of aqua blue for both dining_chair and dining_table). Unlike DiffuScene, our color palette is also unified across room types (i.e. we use the same palette for all room types vs having separate colors palettes for bedroom and living/dining room).

Table 9. Comparison of ATISS [27], DiffuScene [39], and LayoutGPT [8] using semantically rendered scenes generated with our colour palette against the colour palette used in DiffuScene, and using textured assets. All scenes were generated using default settings from prior work and rendered with a square floor plan with simple-3dviz.

			Bedroom			Dining room			Living room		
Coloring	Method	FID↓	KID↓	SCA%	FID↓	KID↓	SCA%	FID↓	KID↓	SCA%	
C	ATISS	71.58	5.65	87.56	59.33	13.22	82.07	57.84	15.35	80.39	
Semantic DiffuScene palette	DIFFUSCENE	32.98	0.49	54.16	45.79	0.86	49.37	45.37	0.81	51.67	
Diffuseene palette	LAYOUTGPT	71.33	4.81	98.73	57.51	13.47	71.93	59.74	14.78	79.90	
Comontio	ATISS	70.68	24.87	94.45	72.79	21.35	90.73	78.33	24.88	91.44	
Semantic Our new palette	DIFFUSCENE	34.52	1.12	58.01	49.69	0.51	49.86	50.10	0.45	53.41	
Our new palette	LAYOUTGPT	57.73	23.33	93.08	57.64	8.35	84.24	60.96	8.38	83.03	
	ATISS	83.12	2.21	57.02	77.69	8.72	74.02	72.61	10.72	67.29	
Textured	DIFFUSCENE	46.55	0.34	50.43	63.03	0.39	44.43	60.27	0.47	48.75	
	LAYOUTGPT	100.85	17.34	99.70	115.34	36.90	95.61	91.86	28.13	99.89	

dering, whether textures or semantic coloring are used, and the precise semantic coloring palette used. To check the impact of each of these choices on the evaluation metrics, we conduct a series of experiments. For these experiments, we generate and save a thousand scenes (for each roomtype) for each method with official pretrained checkpoints, and then vary the rendering style based on the experiment. Thus, the scenes are kept constant with just the rendering style being changed.

Experiments here use *per-roomtype* models (i.e. separate models trained for bedroom, dining room, and living room) except for LayoutGPT.

Table 10. Comparison of rendering with simple-3dviz vs our rendering tool (STK) in different settings, which supports rendering of arbitrary floor shapes. Scenes are generated without any conditioning using official pretrained models (separate models are used for each room type). As original DIFFUSCENE [39] cannot generate with floor conditioning, we use a square floor for the generated scenes. We compare rendering the GT with the actual floorplan or the square floor, and rendering with different scales.

			Bedroom			Dining room			Living room		
GT	Renderer	Scale	FID↓	KID↓	SCA%	FID↓	KID↓	SCA%	FID↓	KID↓	SCA%
square	simple-3dviz	Fixed	34.52	1.12	58.01	49.69	0.51	49.86	50.10	0.45	53.41
square	STK	Fixed Zoomed-in	68.01 58.80	1.45 5.08	71.50 86.67	45.18 41.96	3.33 4.93	66.09 85.67	44.27 39.34	5.83 5.88	71.11 82.42
actual	STK	Fixed Zoomed-in	75.79 100.90	15.65 47.96	100.00 99.94	79.86 141.03	41.82 108.74	99.99 98.35	77.41 121.78	44.78 103.92	99.99 99.19

Impact of rendering style. Prior work has used different types of renderings for evaluation, including top-down semantic classes [39], top-down textured [27], and perspective textured [8]. In our experiments, we use the top-down birds-eye-view as it provides a more holistic view of the scene. Prior work also typically does not include the floor and architecture elements as part of the rendering. As our work focuses on whether the objects are correctly placed on the floor, we compare how the evaluation metrics change depending on whether the floor is included in the rendering or not. For this initial investigation of the rendering style, we use a square floor (filling up the entire image) to see how much including the floor impacts the evaluation metrics.

We also notice that the semantic coloring used by DiffuScene does not visually group similar categories together. Thus, we also compare the impact of using a different semantic color palette for evaluation. In our revised color palette, we choose similar colors for object categories that are semantically closer together (e.g. can be grouped into a coarser category). See Fig. C.2 for examples of scenes rendered with the new color palette vs the original color palette, and Fig. C.3 for the correspondence between colors and semantic object classes.

As some prior work used textured assets, we also investigate how using textured vs semantic top-down rendering affects the metrics for DiffuScene in Table 8. We report only FID, KID, and SCA, as these are the metrics impacted by the rendering style. We see from Tab. 8 that the view-based metrics are indeed affected, with higher FID and lower KID when a square floor is included.

Does rendering style affect evaluation of methods in prior work? In Table 9, we check how the semantic colorings and using textures affect the ordering of different methods. We compare ATISS [27], DiffuScene [39], and LayoutGPT [8].

Colour palette for semantic rendering. With our revised semantic palette, we find LayoutGPT performance to be more clearly separated (and comparatively better) than that of ATISS.

Textured vs semantic rendering. Overall, with semantic renderings, the FID is consistently lower and the KID consistently higher. With the FID and KID, the relative rankings of the methods are the same.

Comparing rendering with simple-3dviz vs STK. We also compare rendering with a square floorplan vs the actual floorplan. To allow for rendering with different floor shapes, we develop our own rendering tool that can generate arbitrary floor geometry given the set of corner points. Table 10 reports semantic results with our new color palette only. Switching from simple-3dviz to our STK renderer under the same fixed scale leaves FID/KID almost unchanged but raises SCA slightly. Changing the camera to the zoomedin view (no padding) increases SCA further because larger projected objects are easier to classify, while FID/KID shift only marginally. When the reference images are rendered with the actual, non-square floor shape, FID and KID climb steeply for both scales—an expected penalty because the generated scenes still assume a square outline and thus diverge in floor-pixel distribution.

Impact on SCA. Intriguingly, we find the SCA dramatically increases when we switched to our updated rendering settings, indicating that under this setting, it was easy for the classifier to distinguish between generated and ground-truth scenes.

C.3. SCA analysis

Upon investigating the change in SCA further, we find that the retrieval process results in very limited set of objects being selected for generated scenes, causing the classifier to easily identify which scenes are generated. This was not apparent with the rendering choices in prior work, as the objects are rendered too small and without sufficient details.

We test this hypothesis by plotting a histogram of 3D model IDs used in ground truth vs generated scenes. From Figure C.4, we see that ground-truth bedrooms use a diverse set of object models, whereas DiffuScene relies on a narrow subset, amplifying appearance differences that STK makes more visible. These differences come from the

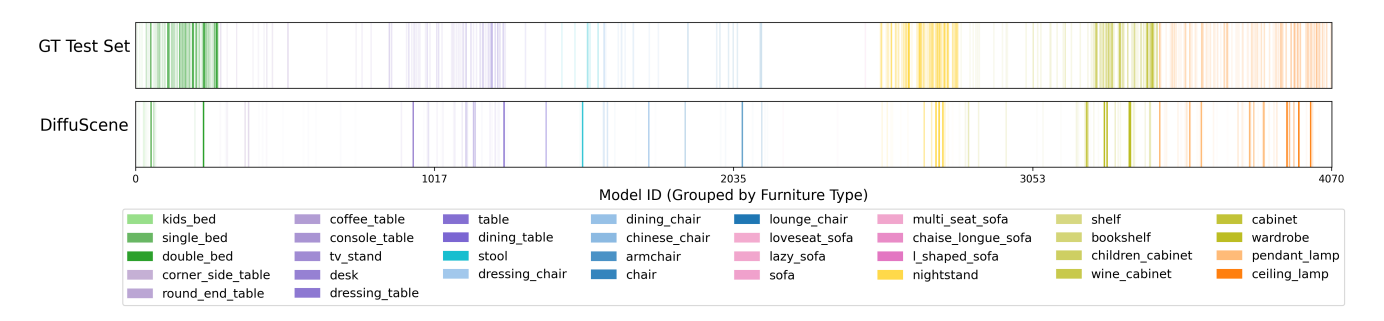


Figure C.4. Model-ID frequency histograms for bedroom. Color intensity indicates how often each model ID (specific object model) appears in the ground-truth test set (top) and in scenes generated by DiffuScene (bottom). Model IDs are grouped by object category, and each category is shown in a distinct colour. The ground truth 3DFront scenes distribute their counts over many model IDs, whereas DiffuScene uses only a small subset, revealing lower shape diversity in its generated results.

Table 11. Accuracy of orientation baselines with 4 classes on z-axis direction with different error thresholds for different baselines.

		Bedroom	1]	Living roc	m	1	Dining roo	m	Ove	rall (avera	nge)
	< 5°	< 10°	$< 45^{\circ}$	< 5°	< 10°	$< 45^{\circ}$	< 5°	< 10°	$<45^{\circ}$	$<5^{\circ}$	< 10°	$< 45^{\circ}$
Random	23.7	24.3	25.0	23.6	23.6	24.6	23.1	23.1	23.5	23.5	23.7	24.4
Majority	38.2	38.3	39.3	34.4	34.4	36.1	34.9	34.9	36.8	35.8	35.9	37.4
Inward	56.4	56.5	56.8	34.4	34.5	36.3	31.8	31.8	33.7	40.9	40.9	42.3
APM	81.5	81.5	82.7	77.1	77.2	80.2	76.5	76.6	79.9	78.4	78.4	80.9
GT	96.2	96.4	100.0	94.1	94.3	98.8	94.1	94.3	98.8	94.8	95.0	99.2

object-retrieval step, which cannot guarantee a similar object model distribution, and show that SCA is an unreliable metric when renderings vary.

SCA using model ID. We also run a simple test experiment to investigate the impact of the model ID on the SCA. Instead of rendered image, we use the set of model ID in the scene to represent the scene. More specifically, we represent scenes using a bag-of-words approach, creating binary vectors where each dimension indicates the presence of a specific furniture model ID. For classification, we use a simple neural network with one hidden layer that learns to distinguish between real and synthetic scenes based on the exact model IDs present in each scene. Our model achieved approximately 99% accuracy when trained on a dataset comprising ground truth training scenes and DiffuScene results, then evaluated on ground truth test scenes and separate DiffuScene results. To verify the model's reliability, we conducted a control experiment by randomizing the splits of only ground truth data for both training and testing. This control test resulted in accuracy around 50\%, equivalent to random guessing, confirming our classifier properly learns meaningful distinctions rather than exploiting dataset artifacts.

D. Additional results

In this section, we present additional results, including an evaluation of our attribute predictor (App. D.1), additional

results for our main model (App. D.2), direct evaluation of the predicted layout (App. D.3), details of mixed condition training (App. D.4), results for per-room type models (App. D.5), comparison against PhyScene (App. D.6), discussion of failure cases (App. D.7), and additional examples of generated scenes from our SEMLAYOUTDIFF (App. D.8).

D.1. Attribute prediction

Baselines for orientation prediction. We compare our attribute prediction model (APM) orientation prediction with several baselines. We note that most objects are oriented parallel to the room coordinate axes, so we simplify the orientation prediction as a classification problem. We compare using a random baseline, vs the most frequent orientation (across all object categories and conditioned on the object category), as well as an inward-facing heuristic. We measure the accuracy of the predicted orientation under different error thresholds. Our trained APM achieves the best performance and outperforms baselines (Tab. 11).

Vertical position and object height prediction. We also evaluate our APM for the vertical position (offset from floor) and object height on the unified test set by computing the mean absolute error (MAE) between the predicted and GT offset and height. We get the offset MAE of 0.13m, and the height MAE of 0.15m. The results show that APM can perform well on the 3D attributes given the 2D info.

Limitations in object attribute prediction and retrieval.

Table 12. Evaluation of how well scenes generated using different methods match the distribution of ground-truth scenes for different room types. We report the FID \downarrow , KID \downarrow , SCA%, and CKL \downarrow with different levels of architecture conditioning: unconditioned (None), conditioned on the floor (Floor), and the architecture map (Arch). **Bold** indicates best results. Our SEMLAYOUTDIFF performs better than other methods in most evaluation metrics across different room types and conditions.

		Bedroom				Dinin	g room			Livin	g room			Overall ((average)		
Condition	Method	FID↓	KID↓	SCA%	CKL↓	FID↓	KID↓	SCA%	CKL↓	FID↓	KID↓	SCA%	CKL↓	FID↓	KID↓	SCA%	CKL↓
	DIFFUSCENE [39]	113.85	61.28	99.26	60.89	137.38	97.16	100.00	3.66	125.15	105.82	100.00	9.55	125.46	88.09	99.75	24.70
Mono	MIDIFFUSION [16]	114.97	52.49	96.88	62.38	107.28	46.19	98.50	21.17	79.38	25.13	96.66	0.69	100.54	41.27	97.35	28.31
None	SEMLAYOUTDIFF (Ours)	103.27	9.80	98.59	31.99	92.70	11.33	92.27	9.52	85.82	11.02	99.41	10.13	93.93	10.72	96.76	17.21
	DIFFUSCENE [39]	103.14	44.75	94.83	61.42	94.79	26.09	91.40	2.33	74.52	19.55	97.08	8.04	90.82	30.13	94.43	23.93
Floor	MIDIFFUSION [16]	106.81	34.39	96.88	48.60	94.11	24.18	98.51	21.18	74.45	20.10	96.42	1.13	91.79	26.23	97.27	23.64
FIOOF	SEMLAYOUTDIFF (Ours)	84.93	12.61	93.05	10.08	87.44	16.72	84.92	4.25	73.01	14.23	91.51	3.63	81.79	14.52	89.83	5.99
	DIFFUSCENE [39]	103.16	47.46	95.49	40.89	87.45	21.14	94.51	8.92	74.79	22.06	95.07	11.47	88.47	30.22	95.02	20.42
Arch	MIDIFFUSION [16]	103.74	32.06	94.58	61.72	95.93	36.47	97.17	43.71	80.87	24.66	94.08	5.48	93.51	31.06	95.28	36.97
	SEMLAYOUTDIFF (Ours)	75.42	5.93	86.81	5.27	70.87	9.97	85.79	4.97	66.90	10.05	88.29	4.10	71.06	8.65	86.96	4.78

Table 13. Evaluation of the physical plausibility of the generated scenes for different room types. We compare out-of-bounds (OOB) ratios at the scene (OOB_S \downarrow) and object level (OOB_O \downarrow), as well as the collision rate (COL \downarrow), and navigability (NAV \uparrow) for the architecture-conditioned model.

		Bedroo	om		Dining room					Living r	oom			Overall (av	erage)	
Method	$OOB_S \downarrow$	$OOB_O \downarrow$	COL↓	NAV↑	$OOB_S \downarrow$	$OOB_O \downarrow$	COL↓	NAV↑	$OOB_S \downarrow$	$OOB_O \downarrow$	COL↓	NAV↑	$OOB_S \downarrow$	$OOB_O \downarrow$	COL↓	NAV↑
DIFFUSCENE [39]	55.10	20.77	37.69	91.98	71.50	30.78	42.65	96.07	72.80	26.53	42.57	94.98	66.47	20.03	40.97	94.34
MiDiffusion	65.25	37.81	33.60	95.25	46.63	30.74	64.62	97.22	70.15	35.44	56.64	96.10	60.68	34.66	51.62	96.19
SEMLAYOUTDIFF (Ours)	13.80	4.00	26.21	93.80	15.80	7.53	5.37	99.36	20.30	8.32	16.82	95.92	16.63	6.62	16.13	96.36

Table 14. Statistics on the number of objects across different room types with architectural conditioning results.

	Bedroom	Dining room	Living room	Overall
DIFFUSCENE	5.03	10.97	9.95	8.65
MIDIFFUSION	5.11	7.31	9.63	7.35
SEMLAYOUTDIFF	4.65	8.23	9.47	7.45
GT (train)	4.96	10.71	11.51	6.40
GT (test)	5.09	11.06	11.49	9.39

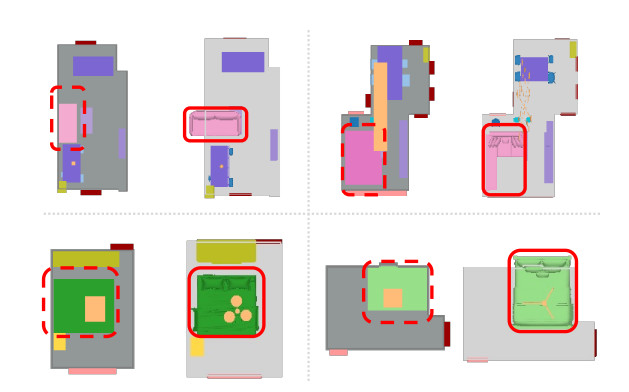


Figure D.5. Failure cases due to poor object attribute prediction and retrieval with our SEMLAYOUTDIFF arch plan conditioning. For each scene, we show the generated semantic map (left) and the final scene after object retrieval (right). On the semantic map, the box (with dashed lines) highlights an object for which the attribute prediction was inaccurate. For the final scene, the red solid line shows the retrieved object (typically with incorrect orientation) due to poor attribute prediction.

Figure D.5 shows the main failure modes that remain after our model produces otherwise accurate 3-D bounding-box layouts. Although the boxes fit the room well, the predicted object attributes—especially orientation—can be wrong. In the top-left scene and the two bottom scenes, beds or tables are oriented unnaturally after retrieval. At the room edges, some objects slide partly outside the plan, and in the top-right example, an L-shaped sofa is distorted because its width and length were swapped during retrieval. These cases show that attribute prediction, rather than box placement, is now the primary source of error.

D.2. Full results for per-masktype model

Evaluation by room type. In Tabs. 12 and 13, we present a comparison of DIFFUSCENE, MIDIFFUSION to our main SEMLAYOUTDIFF model (trained for each different type of conditioning) with breakdown for each room type. Across the three room types, our SEMLAYOUTDIFF outperforms the other methods for almost all metrics, with DIFFUSCENE having the best CKL for dining rooms, and MIDIFFUSION having the best CKL for living rooms when conditioning on no arch or just the floor mask.

Statistics of generated scenes. As the plausibility metrics (e.g., out-of-bounds, collisions, navigability) are affected by the number of objects in the scene, we provide in Tab. 14 the average number of objects in scenes generated by different methods (with architecture conditioning) across different room types. We see that on average, DIFFUSCENE has the highest number of objects, and that our SEMLAYOUTD-IFF has a comparable number of objects to MIDIFFUSION. Even with a similar number of objects, our SEMLAYOUTD-

Table 15. Evaluation directly on layouts. Results are evaluated on architecture-conditioned generated scenes using semantic 3D bounding boxes, without performing object retrieval. SEMLAYOUTDIFF significantly outperforms other prior methods in the pure layout.

		Bedroom			I	Dining ro	om]	Living roo	om	Ove	erall (aver	age)
Condition	Method	FID↓	KID↓	SCA%	FID↓	KID↓	SCA%	FID↓	KID↓	SCA%	FID↓	KID↓	SCA%
	DIFFUSCENE [39]	87.91	100.47	99.99	93.74	94.59	98.91	98.63	114.35	100.00	93.43	103.14	99.63
Arch	MiDiffusion [16]	73.54	78.79	95.72	71.95	74.83	97.31	80.89	83.74	98.16	75.46	79.12	97.06
	SEMLAYOUTDIFF (Ours)	24.16	14.85	94.58	27.46	10.75	93.49	26.88	16.74	96.48	26.17	14.11	94.85

Table 16. Evaluation (with breakdown for each room type) of distribution match for SEMLAYOUTDIFF under single condition (permasktype) training and mixed condition training.

			Bedroom				Dinii	ng room			Livin	ng room			Overall	(average)	
Condition	Training	FID↓	KID↓	SCA%	CKL↓	FID↓	KID↓	SCA%	CKL↓	FID↓	KID↓	SCA%	CKL↓	FID↓	KID↓	SCA%	CKL↓
None	per-masktype mixed	103.27 76.81	9.80 10.39	98.59 91.20	31.99 6.15	92.70 77.05	11.33 12.14	92.27 93.69	9.52 6.11	85.82 63.67	11.02 11.27	99.41 93.54	10.13 3.85	93.93 72.51	10.72 11.27	96.76 92.81	17.21 5.37
Floor	per-masktype mixed	84.93 79.24	12.61 10.01	93.05 88.00	10.08 6.20	87.44 80.11	16.72 10.89	84.92 83.76	4.25 4.03	73.01 69.37	14.23 10.89	91.51 86.35	3.63 2.92	81.79 76.24	14.52 10.60	89.83 86.04	5.99 4.38
Arch	per-masktype mixed	75.42 78.95	5.93 11.10	86.81 92.29	5.27 6.37	70.87 76.53	9.97 8.72	85.79 89.95	4.97 3.69	66.90 65.33	10.05 9.72	88.29 94.32	4.10 2.77	71.06 73.61	8.65 9.85	86.96 92.19	4.78 4.27

IFF generated scenes with considerably less out-of-bounds and collisions than the other methods.

D.3. Direct evaluation on generated layout

One of the most crucial aspects of indoor scene synthesis is creating a plausible room layout. Therefore, we evaluate layouts directly to better compare model performance. Table 15 presents results obtained by rendering top-down views from each method's pure generated layout with 3D object bboxes (prior to object retrieval) and computing layout metrics. These results show that our SEMLAYOUTDIFF significantly outperforms other methods in generating coherent and realistic layouts.

D.4. Experiments with mixed-condition model

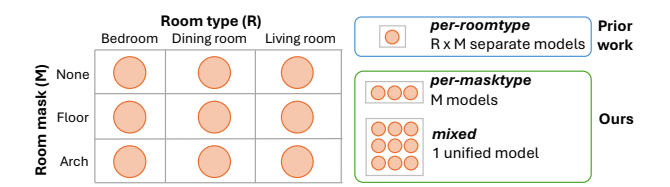


Figure D.6. Prior work [27, 39] typically trained a separate model for each room type and conditioning type. In this work, we explore unified models that combine all room types. Most experiments in the main paper are conducted with per-masktype training, where we train a model for each different type of room mask conditioning (none, floor, arch). We also investigate mixed training with a single unified model.

We propose a mixed condition model that unifies generation with different room mask conditioning: no room mask (none), floor mask, and arch mask within a single framework. During training, each sample randomly selects one of the three condition types with equal probability (1/3). A

condition type indicator (0: none, 1: floor, 2: arch) is introduced as an additional input. It is processed through an embedding layer and MLP to obtain a condition type embedding, which is added to the timestep embedding—similar to the integration of room type embeddings. During inference, the model receives the desired condition type and its corresponding mask: no room mask uses an all-zero mask, the floor mask uses a binary mask (0 for void, 1 for floor), and the arch mask uses a categorical mask (0 for void, 1 for floor, 2 for door, 3 for window). This modification enables a single model to handle multiple room types and varying room mask conditional constraints flexibly.

As shown in Tab. 16, the mixed condition model achieves comparable performance to the per-masktype single-condition model with architecture conditioning, with only slight differences in FID, KID, SCA, and CKL metrics. Notably, the mixed condition model consistently improves results under the no room mask (none) and floor conditions across all room types. For instance, in the None condition, the mixed model reduces the overall average FID from 93.93 to 72.51, KID from 10.72 to 11.27, and CKL from 17.21 to 5.37, while increasing SCA from 96.76% to 92.81%. For the Floor condition, the mixed model also outperforms the per-masktype single-condition model in FID, KID, and CKL. These results indicate that the mixed condition model improves performance under unconditional and floor constraints, while maintaining comparable performance for architecture conditioning.

Tab. 17 presents the comparison of physical plausibility across different condition settings, evaluating both the mixed-condition model and the single-condition models. For the unconditional case, the results show very low OOB values, which is expected since the floor and objects are generated jointly, ensuring boundary consistency.

Table 17. Evaluation (with breakdown for each room type) of the physical plausibility of the generated scenes for SEMLAYOUTDIFF under single condition (per-masktype) training and mixed condition training.

		Bedroom				Dining room					Living r	oom			Overall (ave	erage)	
Condition	Method	$OOB_S \downarrow$	$OOB_O \downarrow$	COL↓	NAV↑	$OOB_S \downarrow$	$OOB_O \downarrow$	COL↓	NAV↑	$OOB_S \downarrow$	$OOB_O \downarrow$	COL↓	NAV↑	$OOB_S \downarrow$	$OOB_O \downarrow$	COL↓	NAV↑
None	per-masktype mixed	4.04 1.30	1.13 0.36	24.72 19.02	93.02 95.70	1.04 0.61	0.13 0.15	14.94 11.90	96.36 97.07	1.04 0.20	0.13 0.02	13.45 12.04	96.52 97.74	2.04 0.70	0.46 0.18	17.70 14.32	95.30 96.84
Floor	per-masktype mixed	12.80 9.60	4.55 3.32	17.84 19.60	95.51 95.08	28.90 25.30	7.51 5.57	11.65 11.99	97.98 97.04	32.10 29.60	8.73 6.31	29.34 12.41	96.57 97.78	24.60 21.50	6.93 5.07	19.61 14.67	96.69 96.63
Arch	per-masktype mixed	13.80 10.40	4.00 3.46	26.21 18.48	93.80 95.86	15.80 26.10	7.53 5.75	5.37 12.60	99.36 97.37	20.30 28.10	8.32 5.73	16.82 12.19	95.92 97.49	16.63 21.53	6.62 4.98	16.13 14.42	96.36 96.91

Table 18. Evaluation of how well scenes generated using different methods match the distribution of ground-truth scenes for *per-roomtype* models conditioned on architecture plan.

		Bedroom				Dining room				Livin	ig room			Overall (average)	
Method	FID↓	KID↓	SCA%	CKL↓	FID↓	KID↓	SCA%	CKL↓	FID↓	KID↓	SCA%	CKL↓	FID↓	KID↓	SCA%	CKL↓
DIFFUSCENE [39]	148.56	75.68	99.61	22.48	88.83	20.89	95.42	11.38	73.70	17.37	94.75	11.00	103.70	37.98	96.59	82.41
MIDIFFUSION [16]	106.32	69.72	99.80	14.46	135.20	92.80	99.03	58.90	89.87	36.43	99.71	59.15	110.46	66.31	99.52	44.17
SEMLAYOUTDIFF (Ours)	156.69	85.00	99.07	7.05	86.72	20.14	95.48	12.13	80.57	23.84	93.70	30.53	107.99	42.99	96.08	16.57

Across floor and arch conditions, the mixed-condition model achieves performance comparable to the single-condition models, with similar or slightly lower OOB and COL values and consistently high NAV scores. This indicates that the mixed model can generalize well across different condition types without sacrificing spatial plausibility, while still benefiting from a unified training scheme.

D.5. Experiments with per-roomtype models

As most prior work on scene generation that learn the distribution of layouts from data are trained so that there is a separate model for each room type (and for each input condition type), we compare the performance of the different methods under this setting.

Results Tabs. 18 and 19 show that SEMLAYOUTDIFF offers the best balance of adherence to the architecture plan and realism. At the scene level, it has lower out-ofboundary (OOB_S \downarrow) errors (14.3% in bedrooms) and keeps them close to MIDIFFUSION for the other room types, while at the object level it gives the lowest $OOB_O \downarrow$ in every room (e.g., 4.5% vs. 11.7% for MIDIFFUSION in bedrooms and 10.0% vs. 17.9% in living rooms). Its overall CKL drops to 16.6, far below MIDIFFUSION 's 44.2 and DIFFUSCENE 's 82.4, indicating the closest match to the ground-truth distribution. Collision rates are lowest in dining (20.2%) and remain competitive in the other rooms, while navigability stays above 94%. Although DIFFUSCENE and MIDIFFU-SION attain lower FID/KID in some cases, SEMLAYOUTD-IFF combines comparable perceptual quality with superior architectural compliance and scene plausibility.

Note that MIDIFFUSION's checkpoint-selection procedure—picking the model with the lowest validation loss—works for floor-plan conditioning but breaks down when we adapt the code to architecture-plan conditioning for bedroom. The "best" bedroom checkpoint consistently

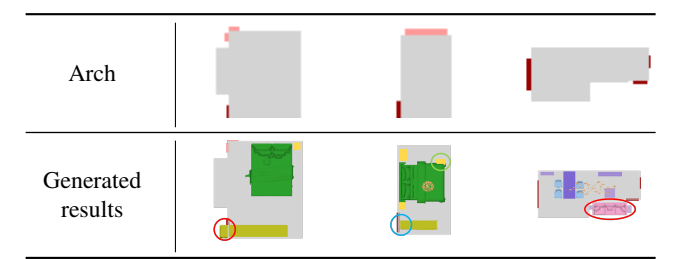


Figure D.7. Examples of failure cases from SEMLAYOUTDIFF-generated scenes with archplan conditioning.

generates scenes filled almost exclusively with kid beds, many placed outside the room boundary. To obtain evaluable bedroom results without otherwise altering MiDiffusion, we therefore inspected several intermediate checkpoints and chose the one that (i) positions furniture at a plausible distance from the room centre and (ii) produces a more varied, realistic mix of bedroom items. Checkpoints for all other room types remain unchanged, preserving alignment with the original MIDIFFUSION protocol.

D.6. Comparision with PhyScene

We also provide a comparison of our SEMLAYOUTDIFF against PhyScene in Tab. 20. However, as the PhyScene training code is not publicly available, we are unable to adapt it to our unified model setting. For comparison, we take the checkpoint provided by PhyScene for living room (the only checkpoint that is publicly available), and we train our model under that setting (single-room type, floorplan conditioning). Compared with PhyScene, our SEMLAYOUTDIFF consistently produces layouts that were more physically plausible with less collisions between objects, and less out-of-bounds errors.

Table 19. Evaluation of the physical plausibility of the generated scenes for per-roomtype models. We compare out-of-bounds (OOB) ratios at the scene (OOB_S \downarrow) and object level (OOB_O \downarrow), as well as the collision rate (COL \downarrow), and navigability (NAV \uparrow) for the architecture-conditioned model.

	Bedroom				Dining room					Living re	oom			Overall (ave	erage)	
Method	$OOB_S \downarrow$	$OOB_O \downarrow$	COL↓	NAV↑	$OOB_S \downarrow$	$OOB_O \downarrow$	COL↓	NAV↑	$\mathrm{OOB}_S\!\downarrow$	$OOB_O \downarrow$	COL↓	NAV↑	$\mathrm{OOB}_S\!\downarrow$	$OOB_O \downarrow$	COL↓	NAV↑
DIFFUSCENE [39]	57.00	21.66	21.61	91.18	71.90	35.05	37.96	95.70	76.10	33.75	29.66	95.51	68.33	30.15	29.74	94.13
MiDiffusion [16]	15.50	11.72	68.56	97.69	14.50	28.82	72.13	99.23	32.00	17.92	82.68	97.39	20.67	19.49	74.46	98.10
SEMLAYOUTDIFF (Ours)	14.30	4.47	22.61	97.11	34.00	12.15	20.22	94.12	32.60	10.04	26.53	94.10	26.97	8.89	23.11	95.11

Table 20. Comparison with PhyScene for the living room with floor condition. Most of the scenes generated using PhyScene have out-of-bounds (OOB) issues, indicating that the objects are not placed within the provided floor mask.

		Dist	ribution			Plausibil	lity	
Method	FID↓	KID↓	SCA%	CKL↓	$OOB_S \downarrow$	$OOB_O \downarrow$	COL↓	NAV↑
PhyScene [49] SEMLAYOUTDIFF	73.50 68.26	13.30 7.65	95.52 92.13	0.99 3.52	84.50 26.50	38.86 6.53	34.44 24.57	95.54 96.24

D.7. Discussion of failure cases

Figure D.7 shows several cases where there are issues with scenes generated by our SEMLAYOUTDIFF. First, objects can be placed outside the room boundaries (first and third images), primarily due to inaccurate attribute predictions (e.g. incorrect object size or orientation). Second, generated objects sometimes block doors, likely because the model lacks explicit constraints or losses to penalize placements near doors. Lastly, redundant objects may appear (middle image, extra nightstand) due to residual noise in the semantic map generated by the diffusion model, which the subsequent attribute model does not effectively eliminate.

D.8. Additional qualitative results

Floor conditioning results. We provide floor conditioning results comparison with the unified models in Fig. D.8. We showcase our model's ability to fit to unusual custom floor masks in Fig. D.9.

Additional renderings. We provide additional renderings of scenes generated by SEMLAYOUTDIFF under architectural plan conditioning. Figure D.9 also shows our model's ability to fit to unusual custom arch masks. Figure D.10 shows top-down orthographic renderings using the same rendering setup as for quantitative evaluation. Additionally, we provide more top-down perspective renderings in both semantic colors (Fig. D.11) and textured (Fig. D.12) to better show the generated 3D layouts.

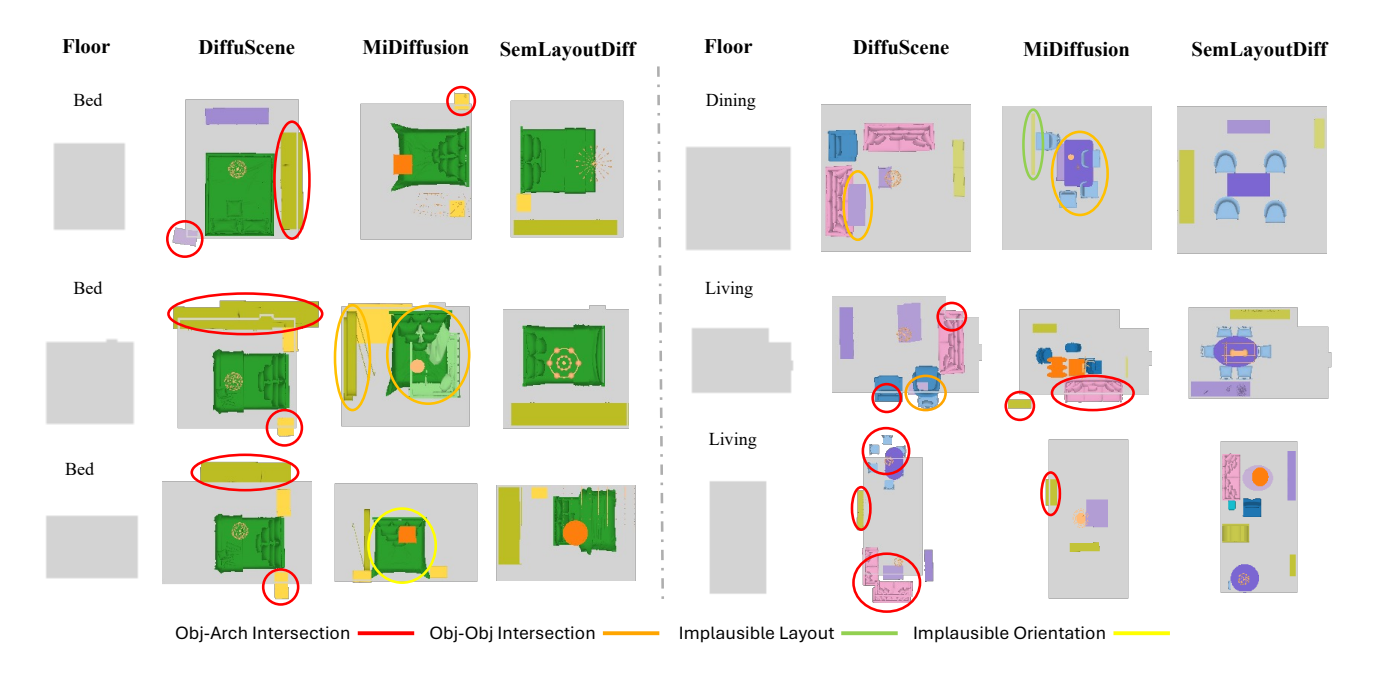


Figure D.8. Comparison of generated scenes using different unified methods with floor conditioning. The left four columns show bedroom scenes; the right four show living and dining room scenes.

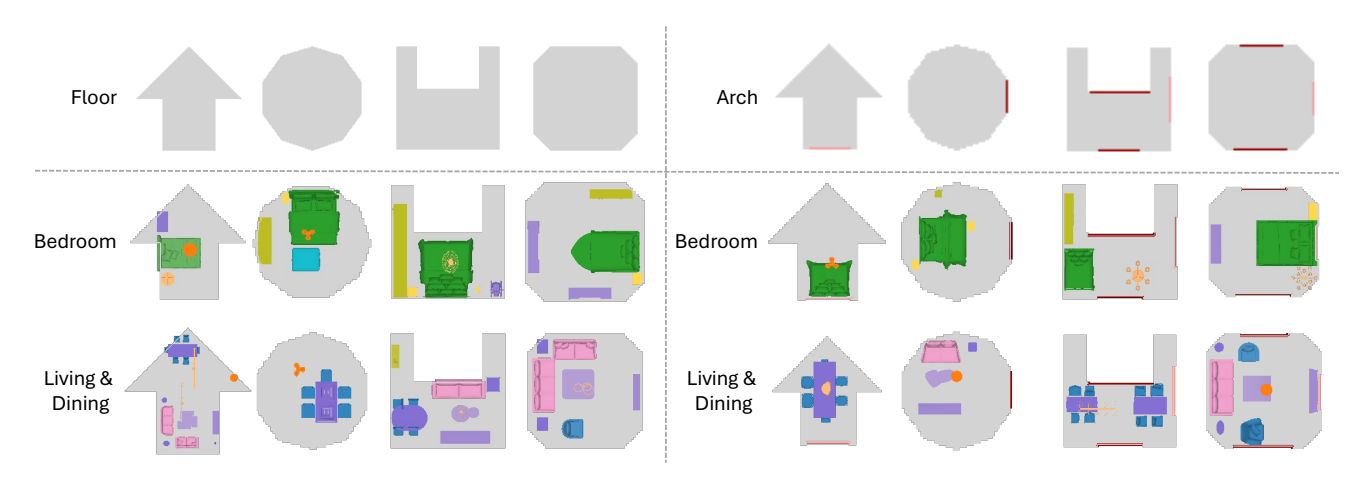


Figure D.9. Examples of generated scenes using our SEMLAYOUTDIFF mixed-condition model under custom floor and arch conditions.

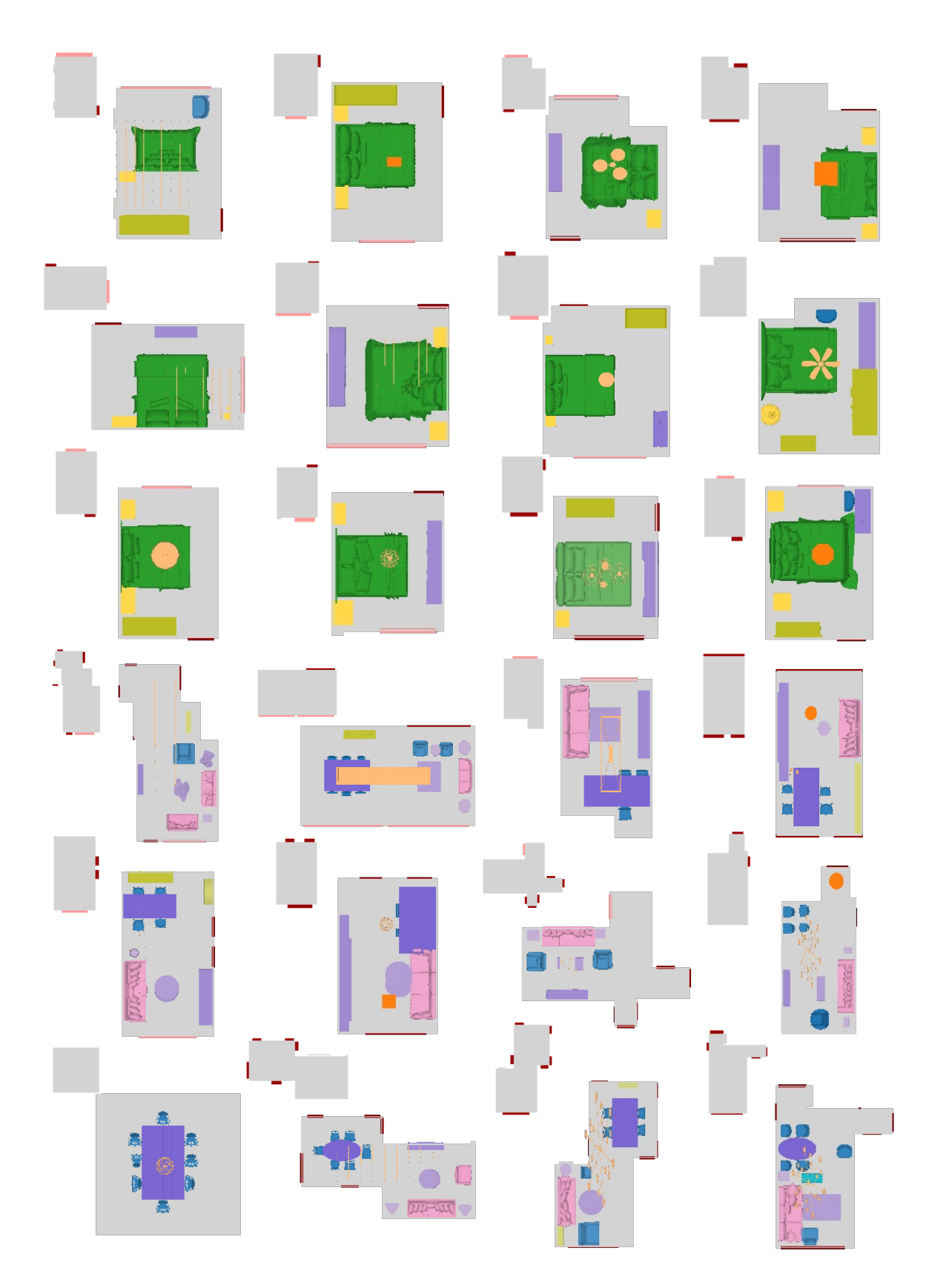


Figure D.10. Examples of architecture-conditioned generated scenes using our SEMLAYOUTDIFF with orthographic rendering as used for evaluation. The condition arch mask is shown at the top-left of each result.

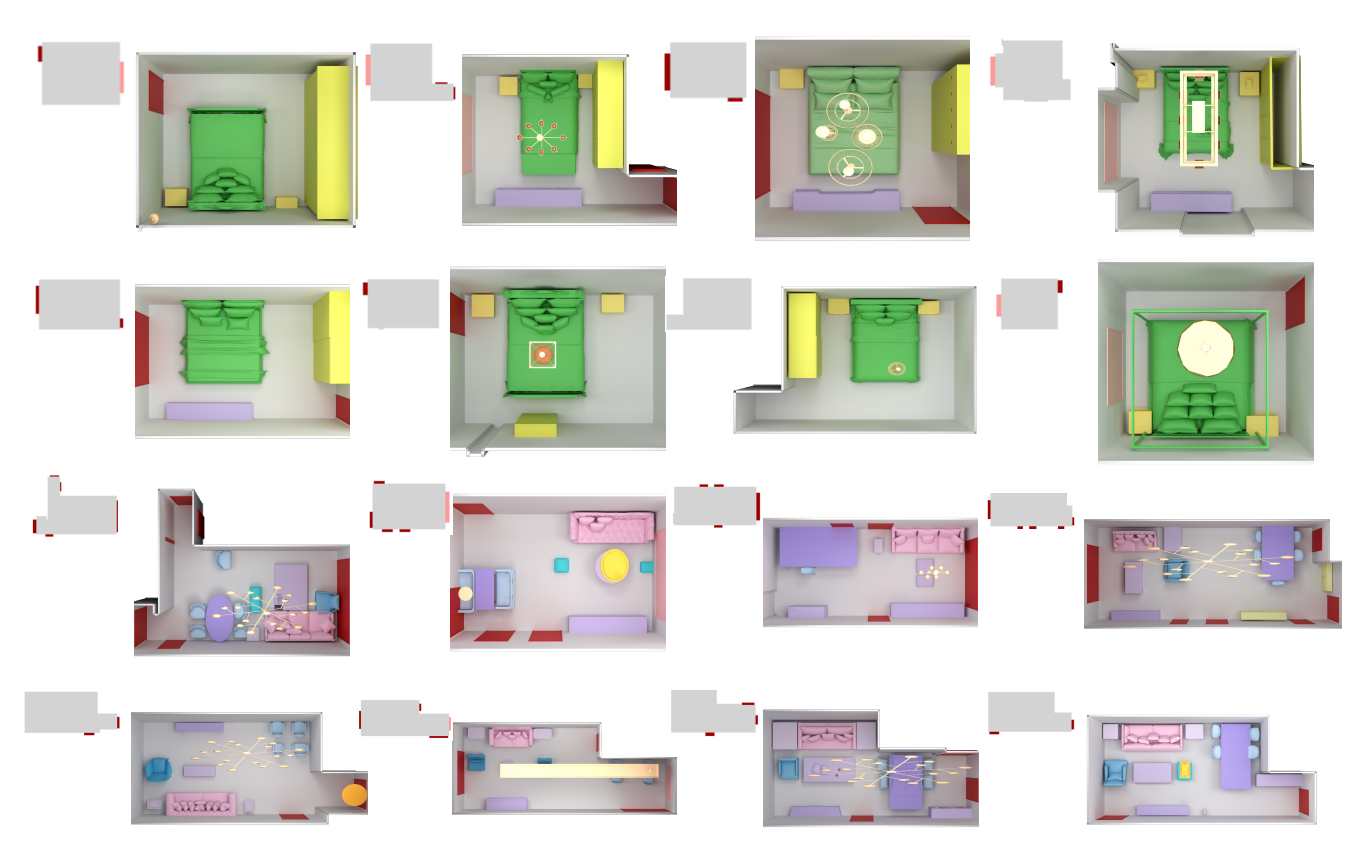


Figure D.11. Examples of architecture-conditioned generated scenes using our SEMLAYOUTDIFF from top-down view with Blender rendering. The top left of each room is the provided arch mask condition.

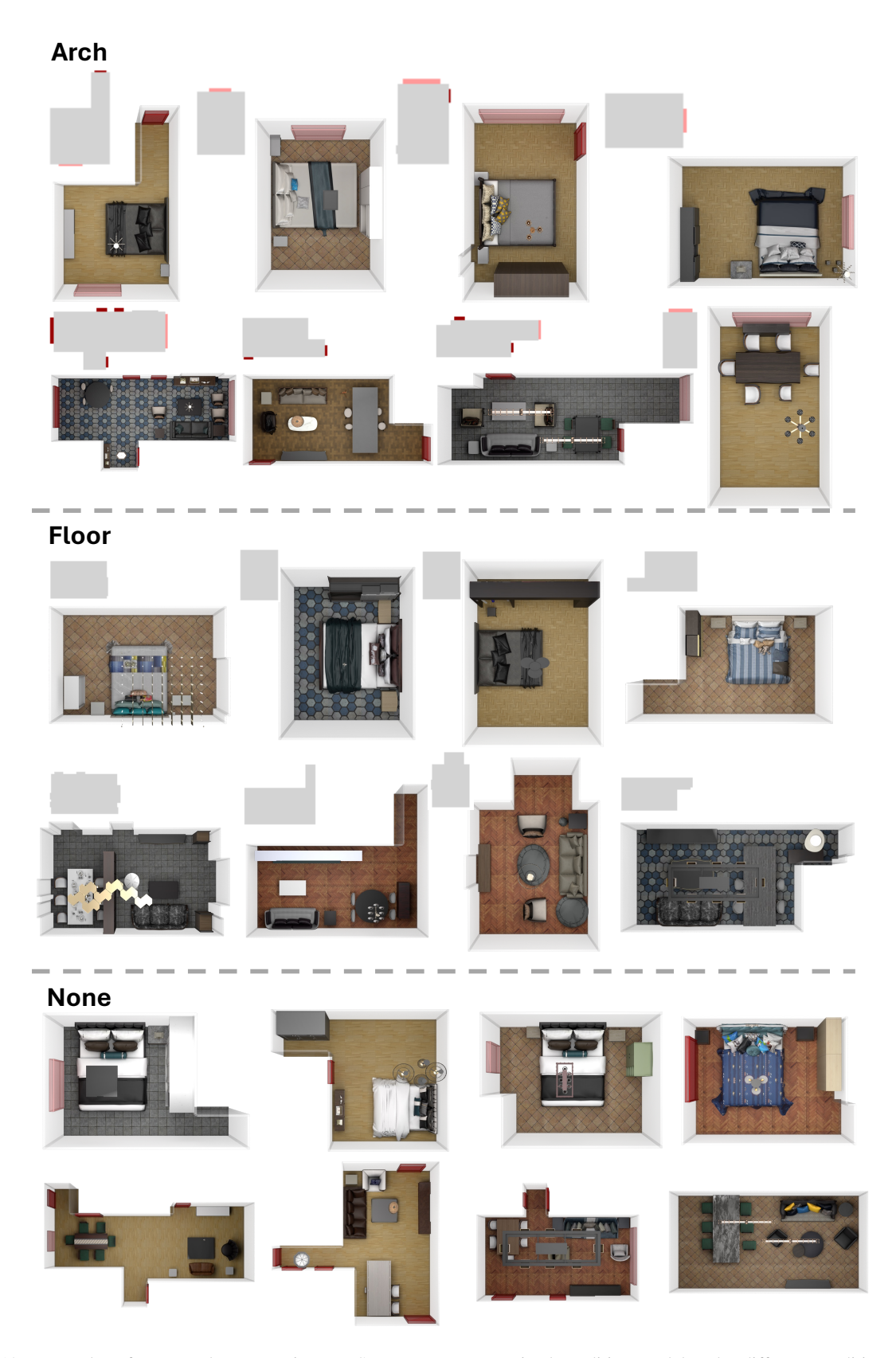


Figure D.12. Examples of generated scenes using our SEMLAYOUTDIFF mixed-condition model under different condition types from top-down view with Blender rendering.